AD-A034 002 AIR FORCE INST OF TECH WRIGHT-PATTERSON AFB OHIO SCH--ETC F/G 20/12
DETERMINING IMPURITIES IN GALLIUM PHOSPHIDE BY ANALYZING CATHOD--ETC(U)
DEC 76 J C SLAVICEK

UNCLASSIFIED GEP/PH/76-9 NL

1 OF 1
AD A034002

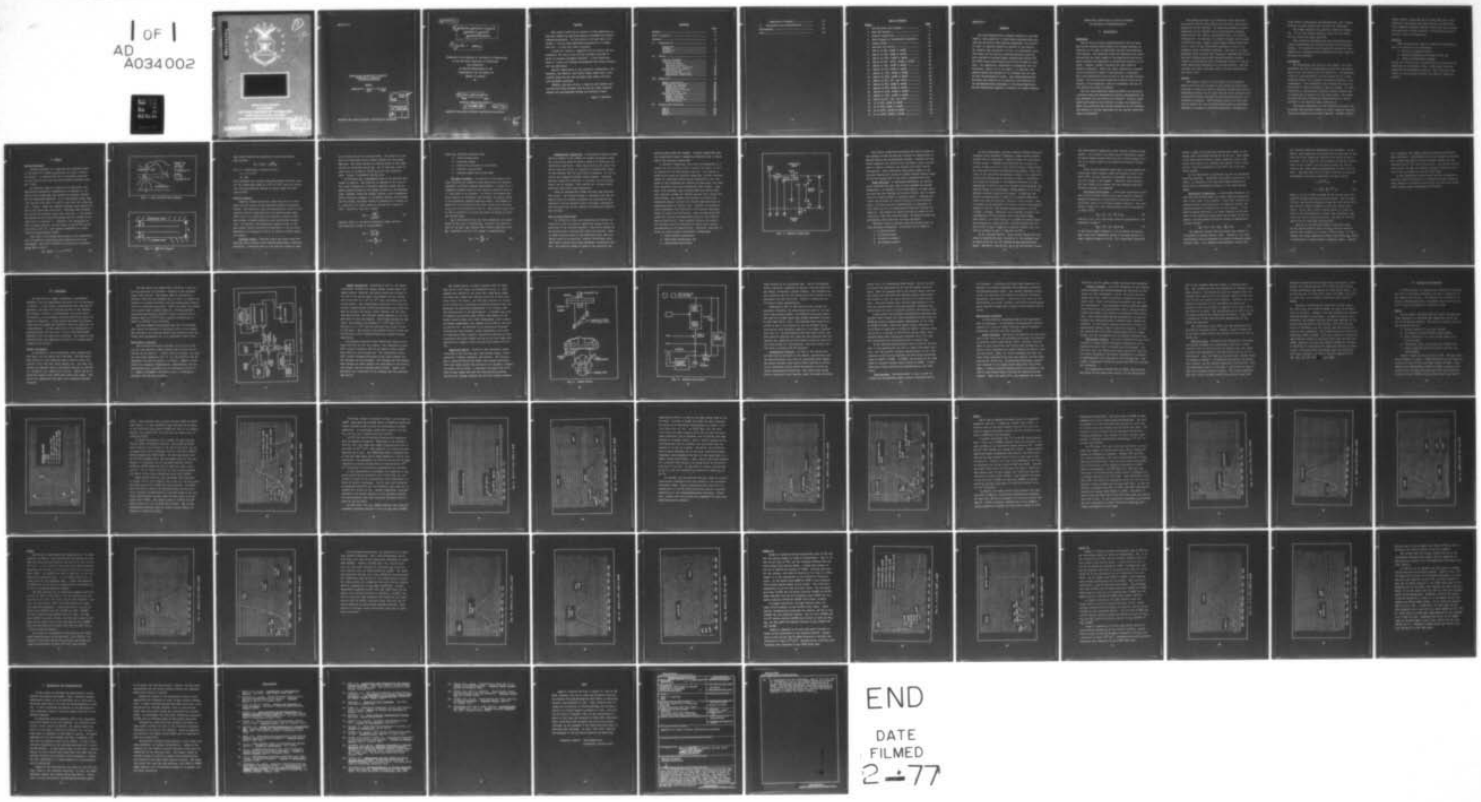

END

DATE FILMED
2-77

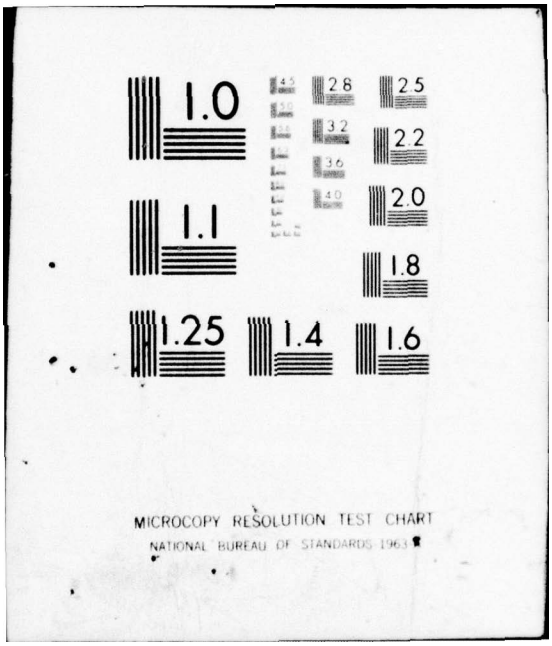
1.0
1.1
1.25
1.4
1.6
1.8
2.0
2.2
2.5
2.8
3.2
3.6
4.0
4.5
MICROCOPY RESOLUTION TEST CHART
NATIONAL BUREAU OF STANDARDS 1963

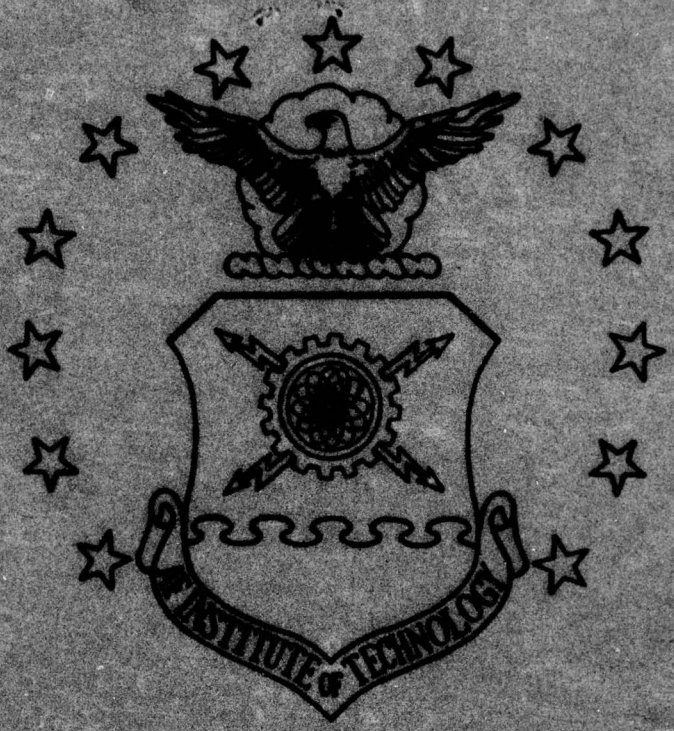

UNITED STATES AIR FORCE
AIR UNIVERSITY

AIR FORCE INSTITUTE OF TECHNOLOGY

Wright-Patterson Air Force Base, Ohio

GEP/PH/76-9

DETERMINING IMPURITIES IN GALLIUM PHOSPHIDE BY ANALYZING CATHODOLUMINESCENCE

THESIS

GEP/PH/76-9 James C. Slavicek
Capt USAF

Approved for public release; distribution unlimited

(14) GEP/PH/76-9

(6) DETERMINING IMPURITIES IN GALLIUM PHOSPHIDE BY ANALYZING CATHODOLUMINESCENCE

(9) Master's THESIS

Presented to the Faculty of the School of Engineering

of the Air Force Institute of Technology

Air University

in Partial Fulfillment of the

Requirements for the Degree of

Master of Science

by

(10) James C. Slavicek B.S.

Capt USAF

Graduate Engineering Physics

(11) December 1976 (12) 76p.

Approved for public release; distribution unlimited

Preface

This report describes my efforts to find impurities in four GaP samples by spectroscopically analyzing the samples' cathodoluminescence. If this report is of any help or interest to the Air Force Materials Laboratory or to Honeywell Inc., it will have been a success.

I thank Dr. Robert L. Hengehold for his advice and his questions, but most of all for his constant optimism in spite of numerous equipment problems. I also thank Maj. Bruce J. Pierce for lending encouragement and advice throughout the experiment.

Special thanks goes to the laboratory technicians, Jim Miskimen, Ron Gabriel, and George Gergal whose help I constantly asked for and who willingly gave advice and help with equipment problems.

Finally, and most of all, I thank my wife Lynette and our son for being tolerant with me and for their constant support and encouragement during the difficult times.

James C. Slavicek

Contents

List of Figures

Abstract

The cathodoluminescence emission spectra of four GaP samples, three grown by a liquid phase epitaxial(LPE) process and the fourth bulk solution grown(BSG), was studied in order to identify impurities present in the samples. The samples were excited by a 20 kV, 1.0 microampere electron beam; and the spectra, photoelectrically detected, were recorded at various sample temperatures between $8^{o}K$ and $100^{o}K$ using liquid helium and liquid nitrogen as coolants. The impurities, identified by comparison with the literature, were S, N, C, Si, and O. In addition, two samples showed the presence of Cu although only one sample was intentionally Cu doped. The cathodoluminescence procedure was found to be as sensitive and effective as the photoluminescence procedure in detecting impurities, and the LPE process appeared to produce the purest samples.

DETERMINING IMPURITIES IN GALLIUM PHOSPHIDE BY ANALYZING CATHODOLUMINESCENCE

I. Introduction

Background

The Air Force Avionics Laboratory(AFAL) and the Space and Missile Systems Office(SAMSO) are working together on detectors to be used in spacecraft attitude and stabilization systems. The detectors sense the radiation from stars and provide the input signal to the associated electronics which maintain the spacecraft's orientation relative to the stars. However, present detectors are only sensitive to infrared radiation. Since the stars' radiation is maximum in the ultraviolet region of the spectrum, a high-gain, low noise preamplifier must be used in the present detector system. If an ultraviolet-sensitive detector could be developed, the preamplifier could be eliminated, and the total system cost would be reduced.

The Air Force Materials Laboratory(AFML) has initiated a program using the semiconductor gallium phosphide(GaP) as the substrate for the ultraviolet detector. However, high-purity GaP crystals are difficult to grow, and impurities alter the electrical and optical properties of the crystals. The effects of various impurities on the crystal properties must be determined.

The general problem is to determine which impurities are present, and how they affect the electrical and optical properties of GaP crystals. To solve this problem, several properties of the crystals can be investigated including conductivity, Hall effect, photoluminescence, and cathodoluminescence. In addition, the crystal samples can be grown in different ways. Using a liquid phase epitaxial(LPE) process, a layer of one crystalline substance is grown on a substrate layer of another substance. The result is large, uniformly doped crystals with "as-grown" surfaces (Ref 21:3). The bulk solution growth(BSG) process produces crystals formed by precipitation from a saturated solution of the desired crystalline substance in a suitable solvent. The BSG crystals are large, uniformly doped, low-flaw-density samples (Ref 21:3).

Problem

The primary purpose of this study was to determine which impurities were present in GaP samples by using spectroscopy to observe an optical property, cathodoluminescence. Cathodoluminescence is the light emitted from a material when electron-hole pairs, produced by striking the material with electrons, recombine. The secondary purpose of this study was to compare the use of cathodoluminescence to photoluminescence as a means of detecting impurities. Several pre-

vious studies investigated photoluminescence, and a sample from one of these studies was included for comparison.

The sample crystals were grown for AFML by Honeywell Inc. Of the four samples studied, three were LPE grown, and the fourth was grown using BSG.

This study was concerned only with determining which types of impurities were present in each of the Honeywell samples. The results do not include the quantity of each impurity or a material profile indicating at what depth impurities were located.

Assumptions

Two assumptions were basic to this study. The first assumption was that the spectroscopic data for the samples would reveal the presence of all impurities. The principal method of investigating the optical properties of a semiconductor sample is to observe its emission spectra at low temperatures. Low temperatures are obtained by using liquid helium or liquid nitrogen to cool the sample. At these temperatures, semiconductor crystals exhibit complex spectra consisting of sharp lines and broad bands. The number of these spectral features and their position is characteristic of the material being investigated.

The second assumption was that sufficient results were available from previous studies to permit impurity identification by comparison of emission spectra. Several spectro-

scopic studies concerning GaP have been made since 1955; therefore, high-purity and doped GaP data was available. Since doped GaP emission spectral lines have been recorded and identified by many observers, the literature formed a reliable source of information.

Criteria

Three criteria were used to compare the experimental data with results in the literature:

1. Position of spectral lines;
2. Relative intensity of spectral lines; and
3. Effect of temperature changes.

All of the criteria were concerned with the wavelength and intensity of the spectral lines. Using these criteria, comparison of experimental spectral lines with those described in the literature yielded the types of impurities present.

II. Theory

Gallium Phosphide

Gallium phosphide is a semiconductor material formed of the Group III element gallium and the Group V element phosphorus. It crystallizes in the zincblende structure in which each Ga (P) atom has four nearest neighbors which are P (Ga).

An important quantity which must be considered when performing luminescence experiments on a material is the width of its energy gap, E_G, between the valence band(VB) and the conduction band(CB). E_G is the minimum energy that a VB electron must have in order to move into the conduction band. Figure 1 shows the reduced Brillouin zone diagram for GaP in two dimensions (Ref 8:52). Brillouin zone diagrams are plotted in momentum space; and, from Fig. 1, the highest VB maximum and the lowest CB minimum are not located at the same value of momentum, k. Therefore, the energy gap for GaP is termed indirect, and the value for E_G at $0^{\circ}K$, $E_G(0)$, is 2.339 ± 0.002 eV. This energy corresponds to a wavelength of approximately 5300Å.

The width of the energy gap depends on the temperature, and two equations relating E_G and temperature have been determined. The first relation was derived by Gershenzon, et al (Ref 11:757):

$$E_G = E_G(0) - 1.7 \times 10^{-6} T^2 \qquad (1)$$

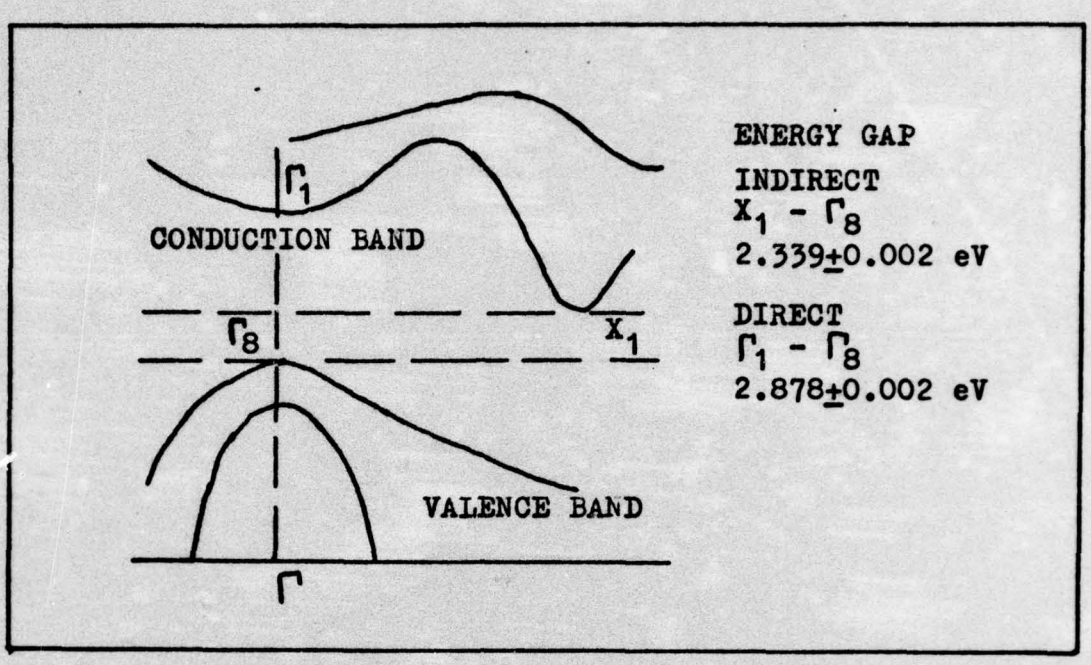

Fig. 1. GaP Brillouin Zone Diagram

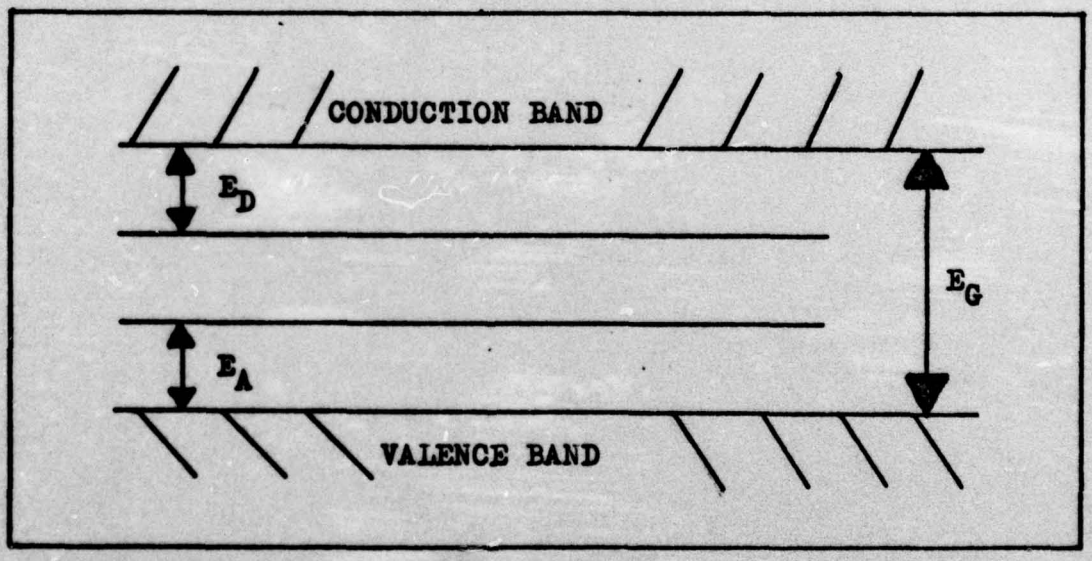

Fig. 2. Band Gap Diagram

The second relation was presented by Panish and Casey (Ref 20:163):

$$E_G = E_G(0) - \frac{aT^2}{(T + B)} \qquad (2)$$

where T = temperature in degrees Kelvin

$a = 6.2 \times 10^{-4}$

B = 460

Both equations were deduced from experimental evidence; and, for the temperature range of 4.2°K to 77°K, both are consistent with experimental results to within 0.01% to 0.02% (Ref 2:1375).

Impurity Centers

Impurity centers are atoms, other than Ga or P, that enter the GaP lattice either substitutionally or interstitially. The impurities that have the greatest effect on the crystal's optical properties are the substitutional type (Ref 14:14), and these will be discussed in terms of electron donors, electron acceptors, and isoelectronic impurities. In addition, the impurities normally found in GaP form simple centers involving a difference of one electron. Therefore, the discussion will be in terms of simple impurity centers.

Electron Donors. Electron donors are atoms which provide one extra electron after bonding requirements have been fulfilled. A Group IV atom on a Ga site or a Group VI atom

on a P site acts as an electron donor. The effect of a donor is to introduce allowed energy levels into the energy band gap. The extra electron is loosely bound to the donor and has an ionization energy E_D. In the band gap, this energy level is located an amount E_D below the conduction band. Figure 2 illustrates the E_D level.

To determine E_D, a hydrogenic model is assumed and Bohr theory is applied. The electron is assumed to be in an orbit, large compared to interatomic spacing, around the impurity center similar to the single electron in the hydrogen atom. However, since the crystal lattice, with a characteristic dielectric constant k, is present between the electron and the center, the orbit radius is increased by a factor of k. Likewise, the total energy is reduced by a factor of $1/k^2$. Therefore, from Bohr theory

$$E_D = - \frac{m_e^* e^4}{2n^2 \hbar^2 k^2} \tag{3}$$

Reducing Eq(3) to the actual hydrogenic model with n=1, the ionization energy is approximately

$$E_D = - \frac{me^4}{2\hbar^2} \frac{m_e^*}{mk^2}$$

$$= 13.6 \frac{m_e^*}{mk^2} \text{ eV} \tag{4}$$

where m_e^* = effective electron mass

m = free electron mass

e = electron charge

k = dielectric constant of the lattice

$\hbar$ = Planck's constant/2π

n = quantum number (Ref 16:267-268)

Electron Acceptors. In contrast to the donors, electron acceptors are impurity atoms which lack one electron necessary to fulfill bonding requirements. A Group II or a transition element atom on a Ga site or a Group IV atom on a P site acts as an acceptor. In effect, the vacant bond site, capable of accepting a VB electron, is loosely bound to the negatively charged impurity center. The energy required for the electron to fill this vacant site, or hole, is E_A and is illustrated in Fig. 2. The allowed energy level for an acceptor is located an amount of energy E_A above the valence band.

E_A is determined using the same assumptions and procedures as were used in finding E_D. However, the effective mass of the hole, m_h^*, replaces the electron effective mass m_e^*. Therefore, for n=1, the energy is approximately

$$E_A = 13.6 \frac{m_h^*}{mk^2} \text{ eV} \qquad (5)$$

Isoelectronic Impurities. Isoelectronic impurity atoms cause no change in the number of valence electrons; Group III atoms on Ga sites or Group V atoms on P sites are isoelectronic impurities. These impurities do not affect the energy band gap unless the impurity is either much larger or much smaller than the host atom it replaces. If the impurity has a smaller (larger) atomic number, a slightly positive (negative) potential is created, and an electron (hole) can be trapped. This results in a charged center which can then bind a hole (electron).

Pairs of isoelectronic atoms can also trap electron-hole pairs. The binding energy is strongest when the impurity atoms are nearest neighbors and decreases as the separation between impurity atoms increases, approaching the limiting value of the isolated isoelectronic impurity. (Ref 25:680).

Recombination Mechanisms

The forbidden energy gap separating the valence and conduction bands can contain additional energy levels as described in the previous section. When GaP is struck by an electron beam, electron-hole pairs are created. Some of these electrons move to the conduction band, and some become bound to an impurity. Optical transitions occur when these electron-hole pairs recombine, releasing a photon. The photon's energy is equal to the energy of the

excited state which has relaxed. Allowed transitions obey the conservation laws of energy and momentum; Fig. 3 illustrates the possible transitions.

A free-free transition, the direct recombination of a conduction band electron with a valence band hole, is rarely observed in the GaP emission spectra. In a direct recombination across an indirect energy gap, crystal momentum cannot be conserved without phonon cooperation, and, compared to the recombinations induced by impurities, the free-free transition has a low probability (Ref 10:399). Likewise, free excitons, free electron-free hole pairs which move together through the crystal lattice with a finite kinetic energy, also require the emission of optical and acoustical phonons in order to conserve momentum while recombining across an indirect gap. Compared to recombinations associated with impurities, free exciton recombinations are also very inefficient. Only in high-purity GaP would free exciton recombinations appear in the emission spectra (Ref 17:29). When impurity centers are present, the primary optical transitions are those which involve recombination at an impurity site. Therefore, from Fig. 3, there are three primary recombination mechanisms:

1. Bound exciton transitions;
2. Free-bound transitions; and
3. Bound-bound transitions.

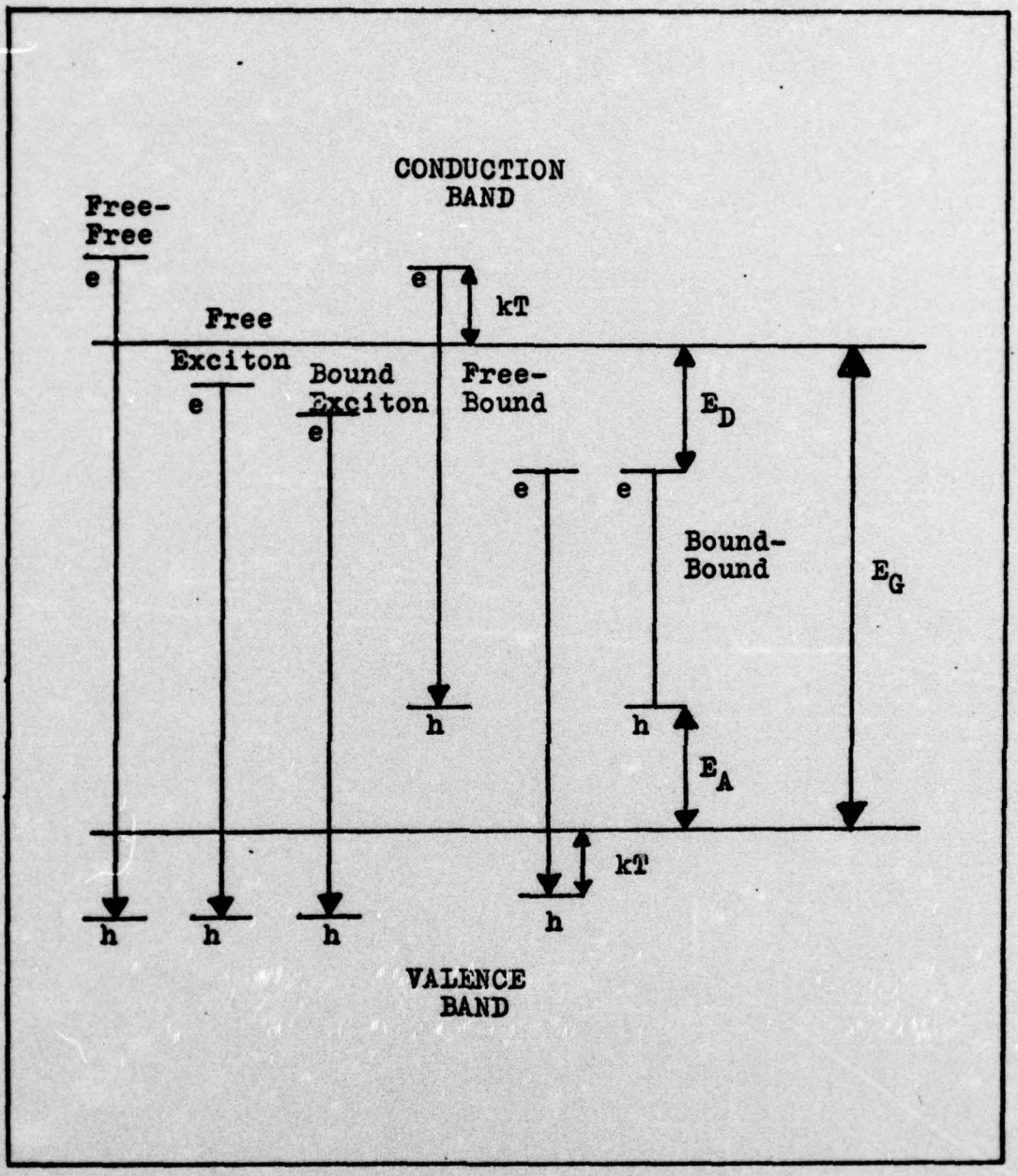

Fig. 3. Optical Transitions

The optical transitions mentioned can also be aided by the crystal lattice through the creation or annihilation of phonons during the recombination process. Phonons with the proper momentum can interact with electrons, holes, and photons to conserve momentum and produce additional allowed transitions. These additional transitions appear in the emission spectra as a series of equally spaced replica peaks on the low energy side of the direct recombination peak.

Bound Excitons. As mentioned previously, an exciton is an electron-hole pair that is held together by Coulomb attraction. In contrast to the free exciton, a bound exciton does not move through the crystal lattice, but is localized at a crystal defect or impurity center. Although excitons can be bound to crystal defects and donor-acceptor pairs, the bound exciton recombinations of importance in this study are due to isoelectronic traps and isolated impurities. The process by which excitons are bound to isoelectronic traps has been described. No binding energy approximations have been made for this situation.

Excitons bound to isolated impurity centers exist in four different situations. An exciton can be bound to

1. A neutral donor
2. An ionized donor
3. A neutral acceptor
4. An ionized acceptor

In this experiment, excitons bound to neutral donors or acceptors were important; therefore, bound exciton recombinations will be discussed in terms of these two situations. In both cases, a hydrogen molecule model can explain the binding energy involved if the exciton binding relationships are expressed in terms of effective mass ratios. Then, the ratio of the exciton's dissociation energy to the impurity's dissociation energy can be written in terms of corresponding ionization energies of the hydrogen molecule or atom. Considering a neutral donor in a material where $m_h^* \gg m_e^*$, the binding energy is $(4.5/13.6)E_D = 0.33E_D$ where 4.5 eV is the hydrogen molecule dissociation energy. If $m_h^* \ll m_e^*$, the exciton binding energy is equal to the energy required to remove the hole and electron, forming a free exciton. This is similar to the hydrogen ion with an electron dissociation energy of 0.75 eV. The exciton binding energy is $(0.75/13.6)E_D = 0.055E_D$. Similarly, for a neutral acceptor, the corresponding binding energies are $0.33E_A$ and $0.055E_A$ (Ref 3:395). Although binding of excitons to neutral donors and acceptors is always possible, neutral donors will not bind a hole if $m_e^* < 1.4m_h^*$; and a neutral acceptor will not bind an electron if $m_h^* < 1.4m_e^*$ (Ref 13:727).

In the emission spectra, bound exciton transitions continue to demonstrate their similarity to the hydrogen atom as shown by Eq (3) and the binding energy approximations above. Therefore, from Eq (3), E_D or E_A has discrete values,

and bound exciton transitions occur between discrete energy states. As a result, the bound exciton transitions appear as narrow peaks located below the free exciton energy (Ref 1: 21) by an amount equal to the appropriate exciton binding energy.

Bound exciton spectral peaks show a strong temperature dependence; sharp emission peaks are usually evident only below 30°K. As the temperature increases, free carriers are less likely to be trapped. Therefore, bound excitons are less likely to be formed, and the resultant spectral features decrease in intensity.

Free-Bound Transitions. A free-bound transition occurs when a free electron (hole) with a mean kinetic energy $\bar{E}_K$ dependent primarily on temperature recombines with a hole (electron) bound to an acceptor (donor) impurity. The transition energy for a free electron-bound hole recombination is (Ref 5:755)

$$E_{FB} = E_G - E_A + \bar{E}_K \pm nE_p \tag{6}$$

Likewise, for a free hole-bound electron recombination, the transition energy is

$$E_{FB} = E_G - E_D + \bar{E}_K \pm nE_p \tag{7}$$

In the above energy equations, n is the number of phonons that assist the transition; and $\bar{E}_K$ is the mean kinetic energy, usually assumed to be kT. If a free-bound transition

occurs, a peak in the emission spectra will appear at the energy value calculated from Eq (6) or Eq (7). Some spread of the free carrier kinetic energy around the value of $\overline{E}_K$ exists and results in a spectral peak broader than a bound exciton peak and symmetrically displaced about the free-bound maximum.

As the temperature is increased, $\overline{E}_K$ and the dispersion about $\overline{E}_K$ increases. Therefore, additional carriers will be freed. An increase of the free-bound peak intensity results with a corresponding decrease of the bound exciton peaks.

Bound-Bound Transitions. A bound-bound transition occurs when an electron bound to a donor impurity recombines with a hole bound to an acceptor. Since this recombination occurs between a particular pair of impurity centers, the resulting spectra is referred to as pair spectra. If the donor-acceptor separation r is large compared to the Bohr radii of the electron at the donor and the hole at the acceptor, the bound-bound transition energy is approximated by (Ref 26:A274)

$$E_{BB} = E_G - (E_A + E_D) + \frac{e^2}{kr} \pm nE_p \qquad (8)$$

The impurity centers have previously been assumed to be located at crystal lattice sites. Therefore, the donor and acceptor will be separated by discrete distances, known as pair radii. In a compound semiconductor, such as GaP,

two different impurity arrangements are possible. In the type I, both impurities are located on the same type of lattice site (both impurities located on Ga sites or both on P sites). In the type II, the acceptors occupy the lattice sites of one element, and the donors occupy the lattice sites of the other compound semiconductor element (Ref 26: A274). The pair radii for the type I and type II impurity arrangements are given respectively by (Ref 26:A275)

$$r = \frac{1}{2} m^{1/2} a_o \tag{9}$$

$$r = \left(\frac{m}{2} - \frac{5}{16} \right)^{1/2} a_o \tag{10}$$

where a_o is the lattice constant of the crystal and m is a positive integer denoting the shell number. For the type II case, the nearest neighbors occupy the first shell (m=1) and the next nearest neighbors occupy the second shell (m=2). In the type I case, certain values of m have no atoms at the corresponding r values; and, therefore, gaps will occur in the emission spectra. The type II emission spectra has no such gaps (Ref 26:A275).

Because of the discrete nature of the pair radii, Eq (8) yields discrete values for E_{BB}; and the emission spectra will consist of a series of sharp peaks. At low r values, the energy separation between consecutive E_{BB} values is sufficient to easily resolve individual peaks. However,

as r increases, the energy separation between consecutive peaks decreases. Individual peaks can no longer be resolved, and a broad band appears in the emission spectra with the resolved peaks on the high energy slope. For phonon assisted transitions, the nE_p term results in phonon replicas appearing in the low energy tail of the broad band.

As the temperature is increased, thermal detrapping of carriers occurs resulting in a decreased emission intensity. Also, because of a smaller value of E_G, the pair band should shift toward longer wavelengths (Ref 15:597).

III. Experiment

In this section, sample information, experimental equipment, and the experimental procedure will be discussed in detail. In this study, cathodoluminescence was used to determine the types of impurities present in GaP samples. Each sample, cooled in a helium dewar, was struck with a 20 kilovolt, 1.0 microampere electron beam which caused the sample to luminesce. A lens system collected the luminescence from the sample and focused it near the input slit of a spectrometer. At the output slit of the spectrometer, a photomultiplier tube was used to detect the luminescence reflected from the spectrometer grating. The output of the photomultiplier was amplified and sent to a recorder which displayed the spectra.

Sample Information

As mentioned in the introduction, three samples were LPE types; and the fourth was a BSG type. The LPE layers were formed on a GaP substrate using a growth charge consisting of Ga, GaP, and, where desired, Cu. The exact procedure and apparatus used in the growth process is outlined in a Honeywell Inc. report (Ref 21:6-9). LPE-67 was an undoped GaP crystal while LPE-68 was doped with copper. Sample #1 was undoped and was grown using Monsanto starting material.

The BSG sample was formed from a solution of GaP in a Ga melt following the procedure outlined in the Honeywell report (Ref 21:4-6). The sample, BSG-12, was used in a previous study and was included here in order to compare the results of cathodoluminescence and photoluminescence experiments for detecting impurities. BSG-12 was grown in a graphite crucible from a sulfur doped G.E. starting meterial. Absorption spectroscopy yielded a sulfur concentration of greater than $3 \times 10^{17} cm^{-3}$ and a carbon concentration of about $1 \times 10^{17} cm^{-3}$ (Ref 21:16,33).

All four samples were mounted such that the electron beam struck the polished or phosphorus side of each sample. This procedure for mounting samples was consistent with the method used by Honeywell in their experiments (Ref 21:10).

Experimental Equipment

The cathodoluminescence equipment used in this study was the same apparatus used by Boulet (Ref 4) with the exception of the detector. Several previous studies also used the same basic apparatus (Ref 22, 6), and therefore all the equipment will not be described in detail. Figure 4 illustrates the equipment schematically. Specifically, the cathodoluminescence equipment will be discussed in terms of the sample environment, excitation source, luminescence detector, and the data recorder.

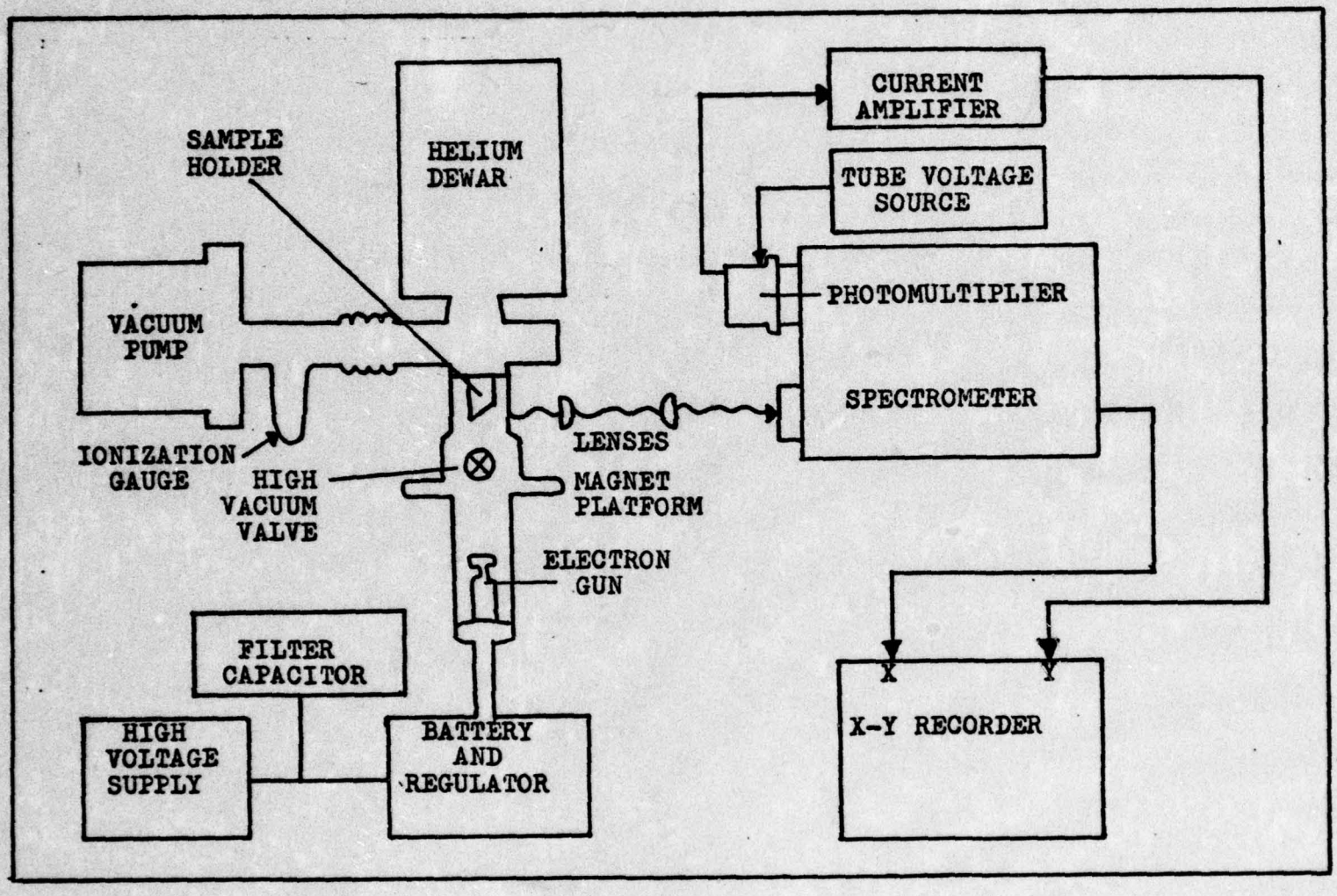

Fig. 4. Block Diagram of Experimental Apparatus

Sample Environment. Referring to Fig. 4, the sample environment included the vacuum system, helium dewar, and sample holder. Briefly, the sample holder was located at the end of the helium dewar cold finger; and the samples were maintained in a 10^{-6} to 10^{-7} torr environment by the vacuum system. The vacuum system consisted of a Welch Scientific Company Series 3102D turbo-molecular pump which was used to evacuate the dewar, sample chamber, and the electron gun chamber. The ultimate vacuum depended on the cryogen used to cool the samples. With liquid nitrogen in the dewar, the pressure was typically 1×10^{-6} torr, while a pressure of 2×10^{-7} torr was produced with liquid helium in the dewar. The pressure was measured using a Varian ionization gauge with a Granville-Phillips ionization gauge controller.

An Andonian Associates Model MHD-30-30N liquid helium dewar was used to cool the samples. For temperatures below $80^{\circ}K$, liquid helium was used in the dewar's inner chamber and helium was the exchange gas. For temperatures above $80^{\circ}K$, liquid nitrogen was placed in the inner chamber and the exchange gas was nitrogen. The exchange gas tube passed down through the inner chamber and terminated in the dewar's cold finger with its attached sample holder. Sample temperatures were controlled by the exchange gas tube pressure (Ref 22:72).

The sample holder, a copper cylinder with its lower face cut at a 45° angle, is illustrated in Fig. 5. Four samples were mounted on the lower face using metal masks; each mask had a small hole through which the electron beam could strike the sample. The 45° angle allowed the samples to be excited by a vertically accelerated electron beam and permitted the resulting luminescence to be incident upon the entrance slit of the spectrometer. A Faraday cup, used to measure the electron beam current, was mounted at the sample holder's base; and a GaAs thermometer, used to measure sample temperature, was located in the side of the holder (Ref 22:77). In addition to the previously mentioned exchange gas tube pressure, sample temperature could also be controlled using a heater. The heater consisted of high resistance wire wound around the end of the cold finger and connected to a Hyperion 30V, 0.6A DC power supply (Ref 22: 72).

Excitation Source. In Fig. 4, the excitation source consisted of the electron gun, high voltage supply, filter capacitor, filament regulator, and battery. The electron gun, a Superior Electronics 5AZP4, was located vertically below the sample holder and consisted of a filament, cathode, two grids, and an anode. A Universal Voltronics BAC 50-16 high voltage supply provided the accelerating potential and also the voltage required for the bias voltage resistor

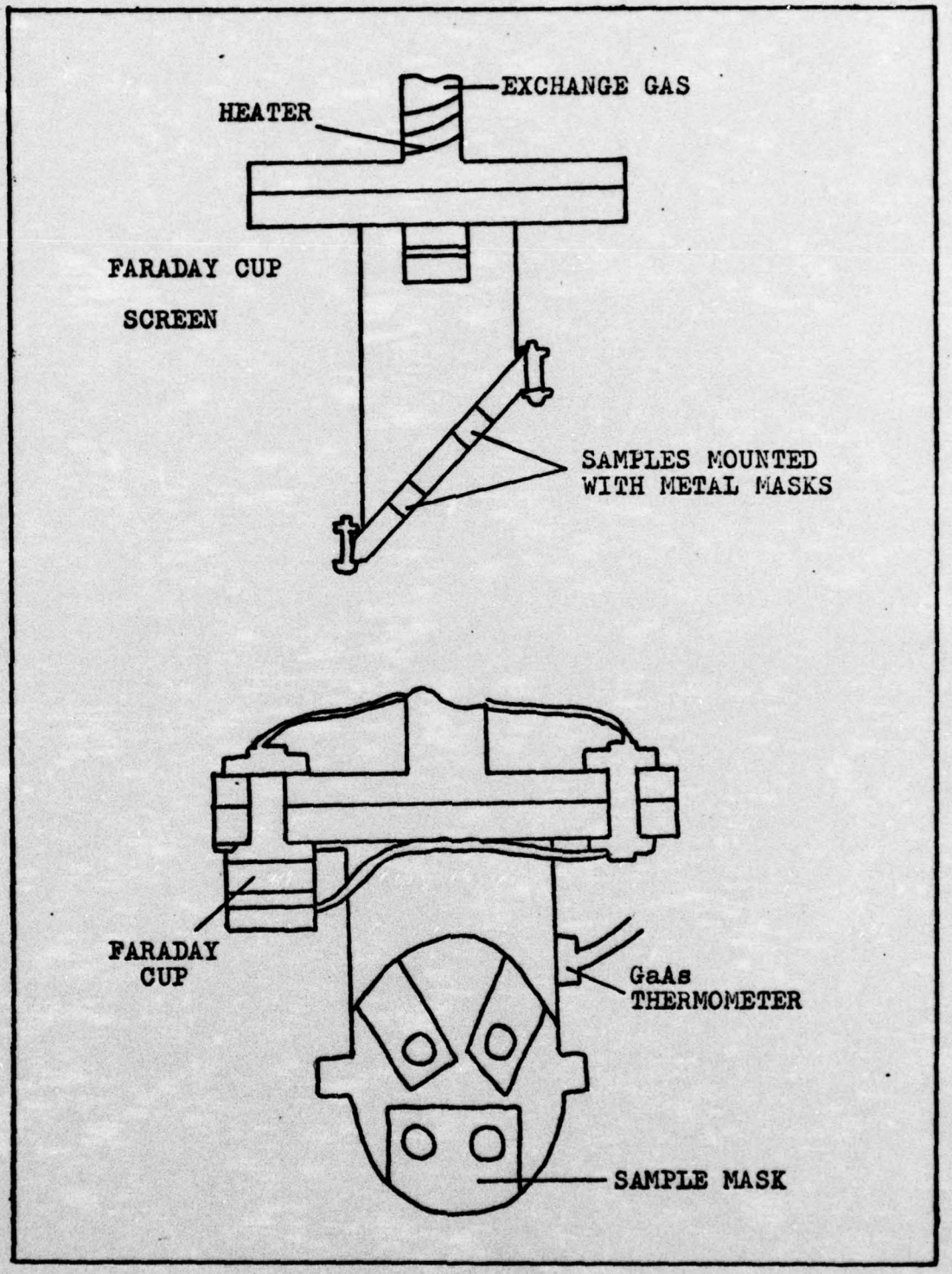

Fig. 5. Sample Holder

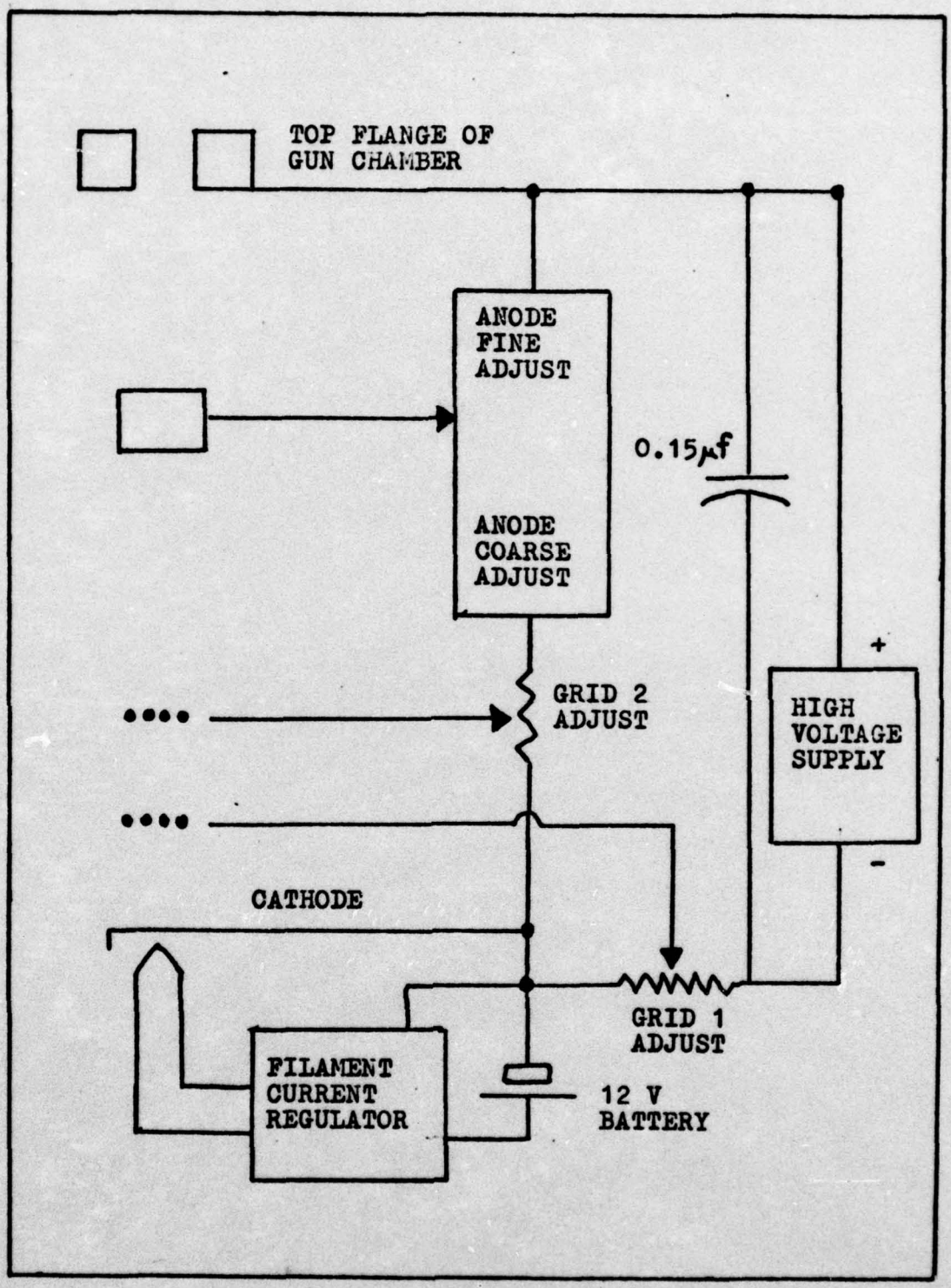

Fig. 6. Electron Gun Circuit

chain located in the plexiglass box. The 0.15 microfarad filter capacitor, connected in parallel with the high voltage supply, maintained a stable voltage. The filament current regulator and the 12V battery were also located in the plexiglass box (Ref 22:73-75). Figure 6 illustrates the excitation source schematically.

Referring to Fig. 6, the positive high voltage was grounded; therefore, the beam energy was equal to the negative high voltage output. The maximum beam energy available was set at 25kV since high voltage breakdown occurred at 27kV (Ref 22:77, 4:21). The electron beam could be directed to any of the samples or into the Faraday cup by positioning small permanent magnets on the magnet platform (see Fig. 4). By adjusting the grid and anode biases, the beam could be focused; and, with the beam directed into the Faraday cup, adjusting the grid biases varied the beam current from cutoff to 5 microamperes. The beam current was read with a Keithley 610A Electrometer.

Luminescence Detector. In Fig. 4, the luminescence detector system consisted of the lenses, spectrometer, and the photomultiplier tube with its associated power supply. The optics included three quartz lenses mounted on an Ealing 50 centimeter optical bench and movable in three mutually perpendicular directions. Two lenses were convex with 10 centimeter focal lengths, while the third was plano-

convex with a 6.5 centimeter focal length. One of the convex lenses was positioned 10 cm from the sample being excited. Near the opposite end of the optical bench, the second convex lens collected the parallel sample luminescence and focused it onto the plane surface of the plano-convex lens. The plano-convex lens, located approximately 6.5 cm from the entrance slit of the spectrometer, dispersed the luminescence in order to slightly overfill the entrance slit.

A Spex Model 1702 3/4-meter Czerny-Turner scanning spectrometer with a Model 1501 1200 grooves/mm grating blazed at 5000Å was used to examine sample luminescence in the range of 5300Å to 8800Å. Spex data showed linear dispersion of 10.85 Å/mm at 5300Å and 10.06 Å/mm at 8800Å. Scanning rates varied up to a maximum of 1000 Å/min, and the Model 1411S straight slits were continuously variable from 0 to 3 mm. The spectrometer was calibrated using a mercury lamp.

An RCA C31025C photomultiplier tube located at the exit slit of the spectrometer was used to detect the sample spectra. The 128 spectral response characteristic of this tube resulted in fairly even response over the entire wavelength range of 5300Å to 8800Å. At 8800Å, the response of the tube began to decrease rapidly toward cutoff at 9000Å. A Fluke 404M power supply provided the photomultiplier with 1000 volts.

Data Recorder. Referring again to Fig. 4, data recording was accomplished using a current amplifier and an

X-Y recorder. A Keithley 4170 Input Head connected to a Keithley 417 Current Amplifier and Picoammeter amplified the photomultiplier output. The current amplifier output became the input for the Y-scale on a Houston Instrument Omnigraphic 2000 Recorder. The X-scale was driven by the spectrometer scan motor through a zero-offset potentiometer which received voltage from a Kepco 6V power supply (Ref 4: 24-26).

Experimental Procedure

In this section, procedures used in this experiment will be discussed. In particular, the procedures used are explained in terms of sample mounting, system alignment, temperature control, and data recording.

Sample Mounting. The method for removing the inner portion of the dewar and the attached cold finger is described in previous reports (Ref 22:74, 4:27). Briefly, with the dewar at room temperature and filled with nitrogen gas, the vacuum valve separating the sample chamber and the gun chamber was closed. Then, the screws fastening the inner and outer dewar portions at the top were removed, and the inner portion was lifted out. As described previously, samples were attached to the sample holder face with small metal masks. A drop of gallium-indium eutectic was placed on the back of each sample before mounting for improved thermal contact. Then, the inner vessel was replaced; the screws

tightened; and the sample chamber and dewar were evacuated.

System Alignment. Since GaP luminesces in the visible, system alignment was straightforward and consisted of both coarse and fine adjustments. First, the lenses were adjusted until some sample luminescence appeared on the entrance slit. Then, the Keithley picoammeter was used for fine adjustments. The wavelengths between 5300Å and 8800Å were scanned with the spectrometer until a strong spectral feature was found; this caused a picoammeter needle deflection. Then, while observing the picoammeter, the lens positions were readjusted until a maximum meter reading was obtained. At this point, maximum luminescence reached the spectrometer grating, and the system was aligned. At sample temperatures above 60°K, luminescence was not always strong; and the picoammeter was the primary alignment tool.

Temperature Control. This study consisted of data measurements at liquid helium (nitrogen) temperatures and at temperatures above that of liquid helium (nitrogen). For the first case, the inner dewar vessel was filled with liquid helium (nitrogen), and helium (nitrogen) at a pressure of approximately 6 psi was used as the exchange gas. Typically, temperatures of 8°K for helium and 78°K for nitrogen were achieved.

For temperatures between 8°K and 80°K, liquid helium was placed in the inner dewar vessel, but the helium pres-

sure in the exchange tube was lowered to approximately 2 psi. The exchange gas was very responsive to changes at the lower pressure. The helium gas flow was stopped, and a mechanical pump connected to the exchange tube by a valve further lowered the exchange tube pressure. Normally, the temperature increased; if not, the heater was activated. A maximum of 24V or 0.5A could be applied to the heater which was rated at 12 watts. For temperatures up to 30°K, the vacuum pump controlled the temperature by itself. Above 30°K, a combination of the pump and short applications of the heater was required.

For temperatures above 80°K, the same procedures were followed as described above. However, liquid nitrogen was in the inner dewar vessel, and nitrogen at 2 psi was the exchange gas.

Data Recording. Recording data consisted of two steps: setting the equipment and collecting a data set. A 20kV electron beam was directed into the Faraday cup; and, using the grid bias adjustments, the beam current was set at 1.0 microampere. Then, the beam was directed onto a sample using the permanent magnets. As described previously, the optics were aligned, and the desired temperature was achieved. With the spectrometer slits 1.0 mm wide, a quick scan was made to find the strongest spectral feature. The current amplifier gain and Y-scale recorder sensitivity were set using this

feature; maximum gain with lowest noise was desired. Typically, the current gain was 10^7 or 10^8, and the initial Y-scale sensitivity was between 0.1 V/cm and 50 mV/cm. The X-scale was set to record full range from 5300Å, just below the band edge, to the point of decreased tube response, 8800Å.

Normally, collecting data consisted of three scans. The first scan, from 5300Å to 8800Å, was made at 500 Å/min with 1.0 mm slits. Usually, this scan recorded all spectral features present in gross form. In order to resolve fine structure, the entrance and exit slits were narrowed to 100 microns and 200 microns respectively. The scan rate was slowed to 200 Å/min, and the current gain and Y-scale sensitivity were readjusted. The X-scale was set to cover full range from 5300Å to 6000Å. This scan recorded in detail the edge emission; mercury calibration lines were included near 5800Å. Finally, the area from 6000Å to 8800Å was recorded at 500 Å/min to investigate the broad band emission in this region. Following these procedures, data was collected, with some exceptions, on each of the four samples at 8°, 15°, 30°, 45°, 60°, 80°, 90°, and 100°K.

IV. Results and Discussion

In this section, the experimental results for each sample will be discussed separately, and then a comparison of the samples will be made. To establish the reliability of using a cathodoluminescence experiment, BSG-12 will be discussed first and compared to a previous study.

BSG-12

In his report, Pritchard (Ref 23) used a photoluminescence experiment to determine GaP impurities; BSG-12 was one of the samples studied. The spectral features detected and discussed were the

1. Sulfur-carbon(S-C) pair band (5610Å),
2. S-C phonon replicas (5735Å, 5860Å, 5990Å),
3. Fine structure on the high energy slope of the S-C pair band,
4. Silicon(Si) donor free-bound peak (5530Å), and
5. Silicon-silicon/sulfur-silicon(Si-Si/S-Si) pair band (6250Å).

Figure 7 shows the initial scan at 8°K. The most prominent feature is a peak at 5600Å identified by its shape and position as the S-C pair band (Ref 9:5638, 19:180). Peaks appearing at approximately 5710Å and 5848Å are phonon replicas of the S-C pair band while the broad band beginning to show at about 6500Å is the Si-Si/S-Si pair band (Ref 9:

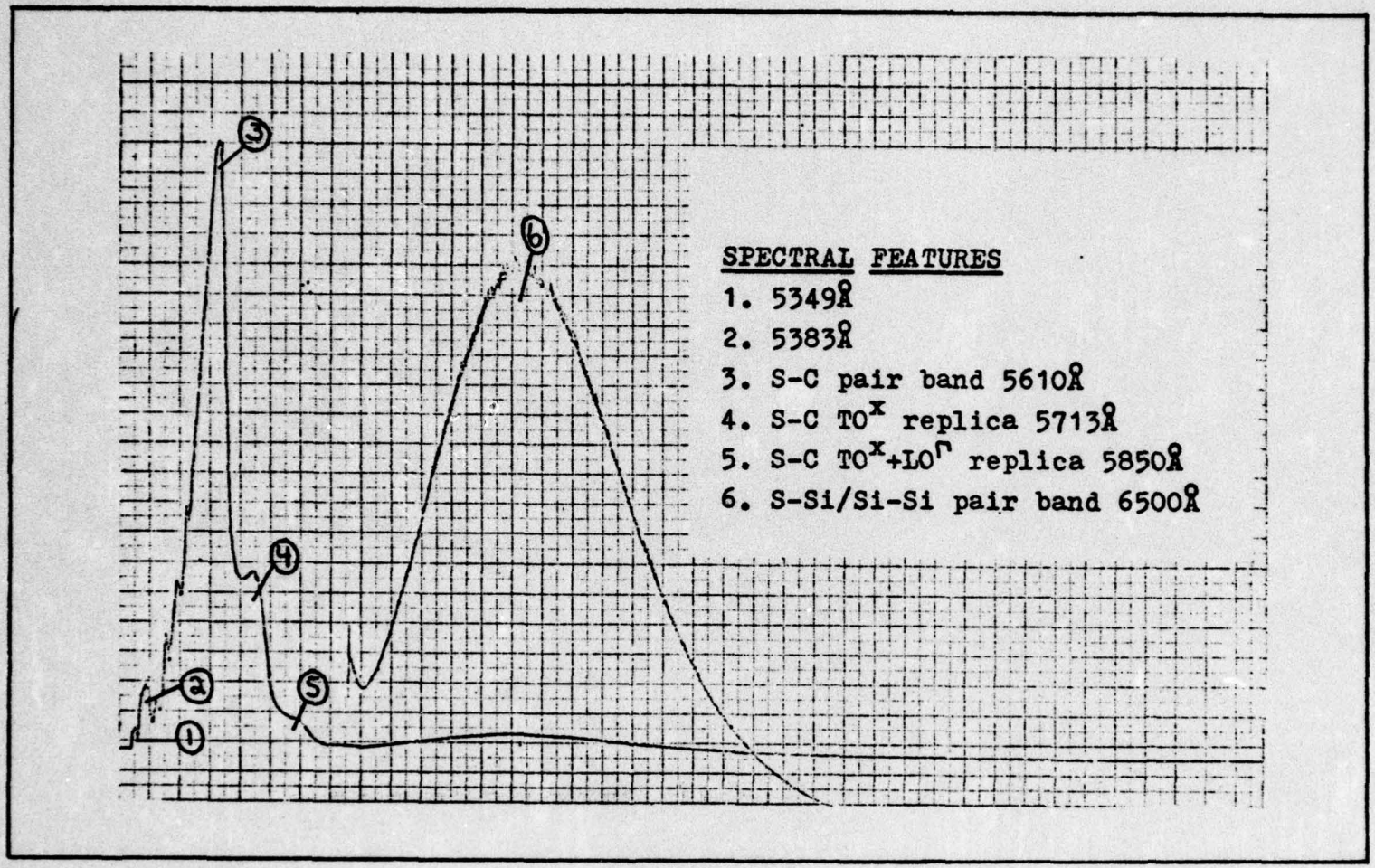

Fig. 7. BSG-12 at 8°K, 5300Å to 8800Å

5638). This peak has been reported between 6200Å and 6500Å (Ref 23:53). In fact, Pritchard also reported the presence of the Si-Si/S-Si pair band at 6500Å for some of his samples. Finally, the initial 8°K scan also has two narrow bands at 5349Å and 5383Å.

At higher resolution, Fig. 8 shows the edge emission between 5300Å and 6000Å for BSG-12. The 5713Å and 5850Å phonon replicas are located 47 meV and 98 meV below the S-C no-phonon peak which identifies them as a TO^X and a TO^X+LO^Γ phonon respectively (Ref 7:660). On the high energy side of the S-C no-phonon peak, the individual peaks of the pair spectra are resolved; and the gap which appears between 5447Å and 5460Å identifies the S-C band as a type I pair spectra. In the type I case for S-C, the carbon acceptors and sulfur donors occupy phosphorus sites (Ref 9:5634).

Below 5400Å (2.30 eV), the individual pair peaks are no longer visible (Ref 9:5637); and in Fig. 8, the previously mentioned peaks below 5400Å have been resolved. At 5352Å, the sharp peak is due to the unresolved pair of lines A-B which represent recombinations of excitons bound to the isolated isoelectronic nitrogen impurity which acts as an acceptor (Ref 7:658). The smaller peak at 5383Å is the TA^X phonon replica of the A-B peak (Ref 10:403). The C line, representing excitons bound to neutral sulfur donors, is present at 5370Å (Ref 7:658).

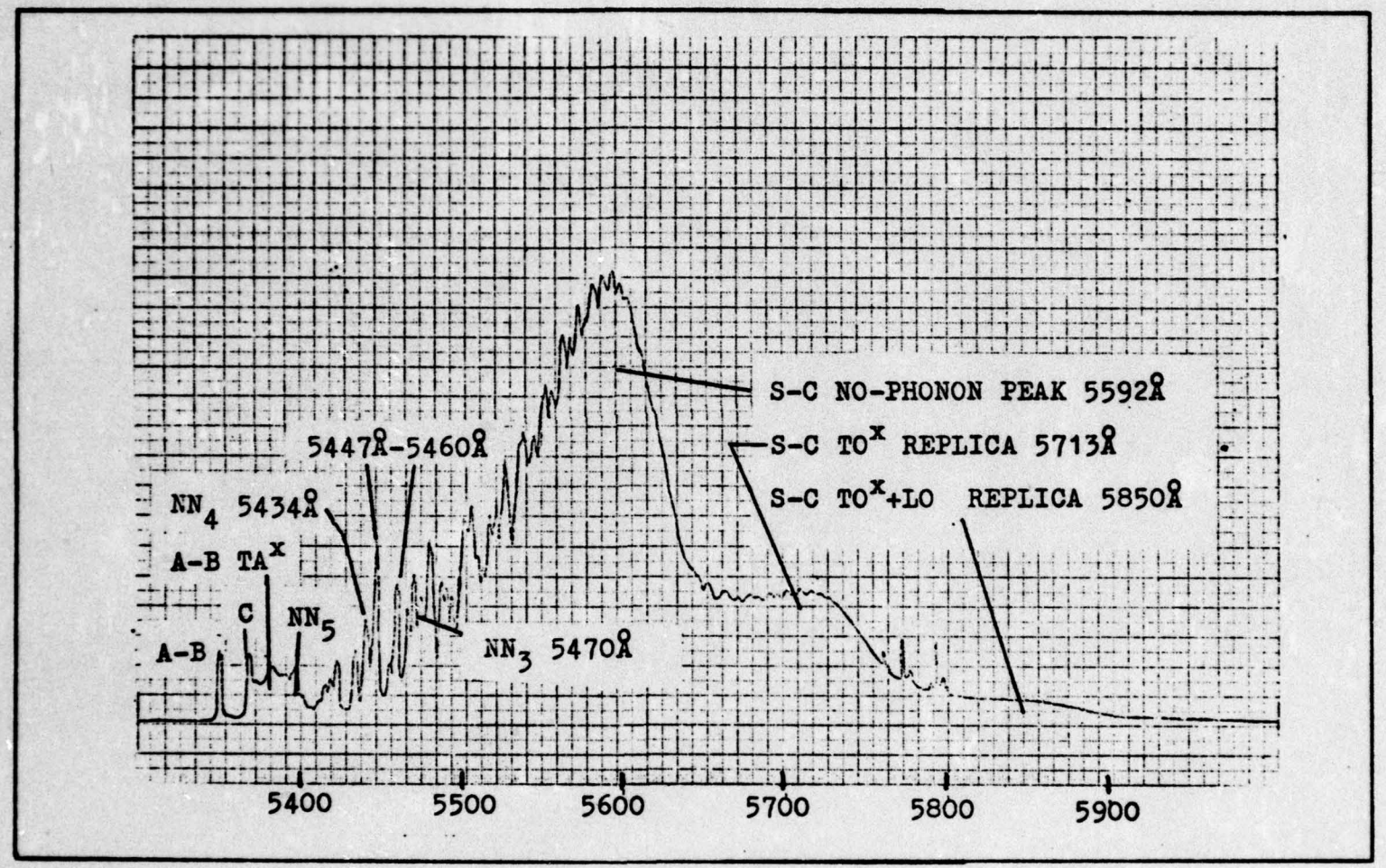

Fig. 8. BSG-12 at 8°K, 5300Å to 6000Å

The final feature of interest in Fig. 8 is the peak at 5398Å. This peak and possibly those at 5434Å and 5470Å represent excitons bound to pairs of isoelectronic nitrogen impurities. In particular, these peaks would be the NN_5, NN_4, and NN_3 peaks respectively (Ref 24:858).

At 8°K, the BSG-12 spectral features are consistent with the sample information. Referring to the Honeywell data (p. 20), the sulfur and carbon concentrations were on the order of 10^{17} cm^{-3}. This resulted in a strong S-C pair band and the C line. The 6500Å broad band is probably due to the S-Si pair band, and is weak because of a low Si concentration. The appearance of both the A-B and the NN peaks indicates a nitrogen concentration of approximately 10^{18} cm^{-3} according to experimental measurements (Ref 24:687).

As the temperature is increased, the intensity of the bound exciton peaks decreased; and at 45°K (Fig. 9), all traces of bound exciton recombination have disappeared because of thermal detrapping. The S-C pair band intensity is unchanged from 8°K, but the S-Si/Si-Si pair band has increased by a factor of two. Further temperature increases resulted in an overall decrease of the spectral features, but the S-Si/Si-Si pair band intensity increased with respect to the S-C band.

At 80°K (Fig. 10), the 6500Å S-Si/Si-Si pair band has a greater intensity relative to the S-C pair band (5610Å).

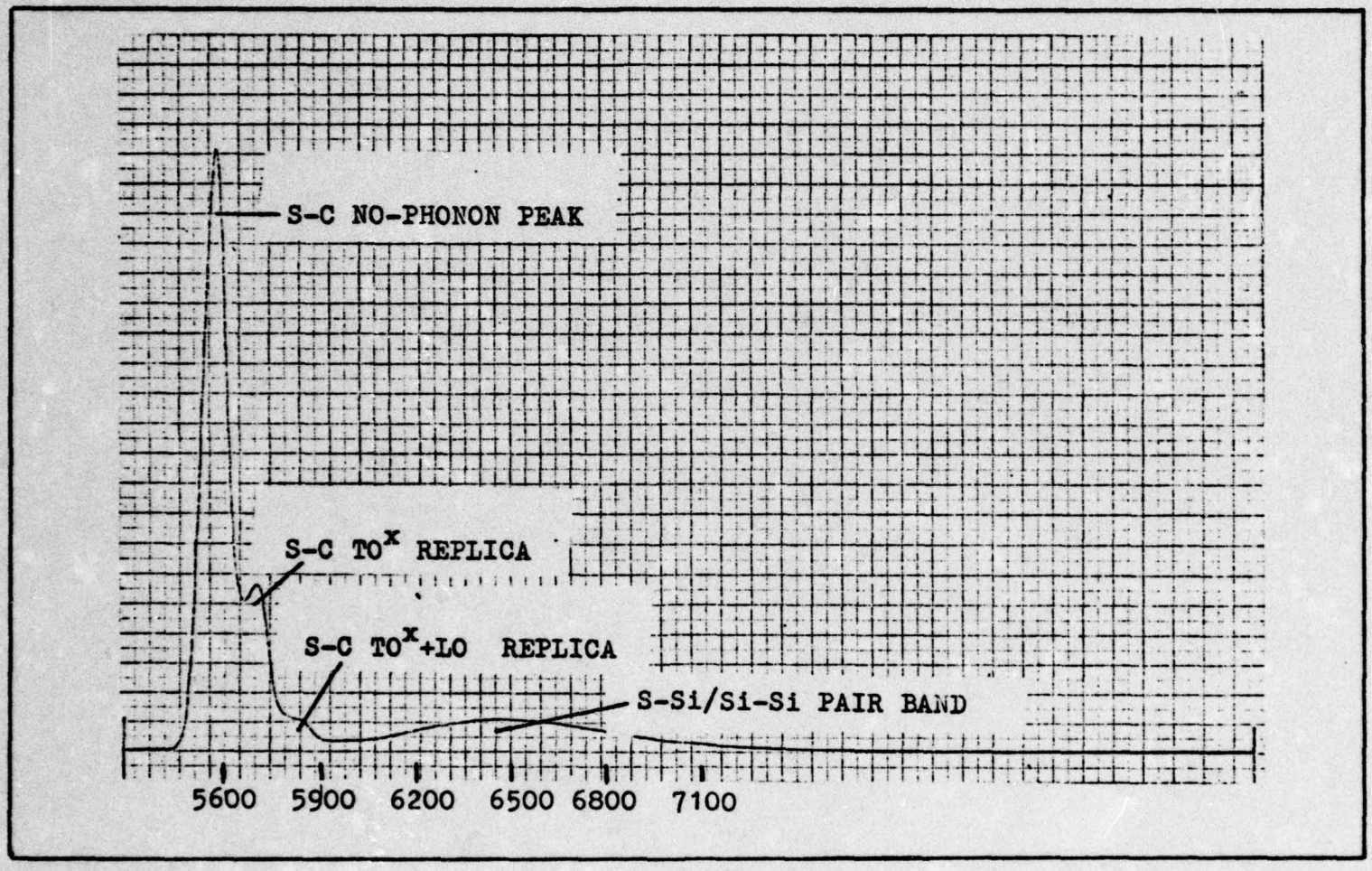

Fig. 9. BSG-12 at 45°K, 5300Å to 8800Å

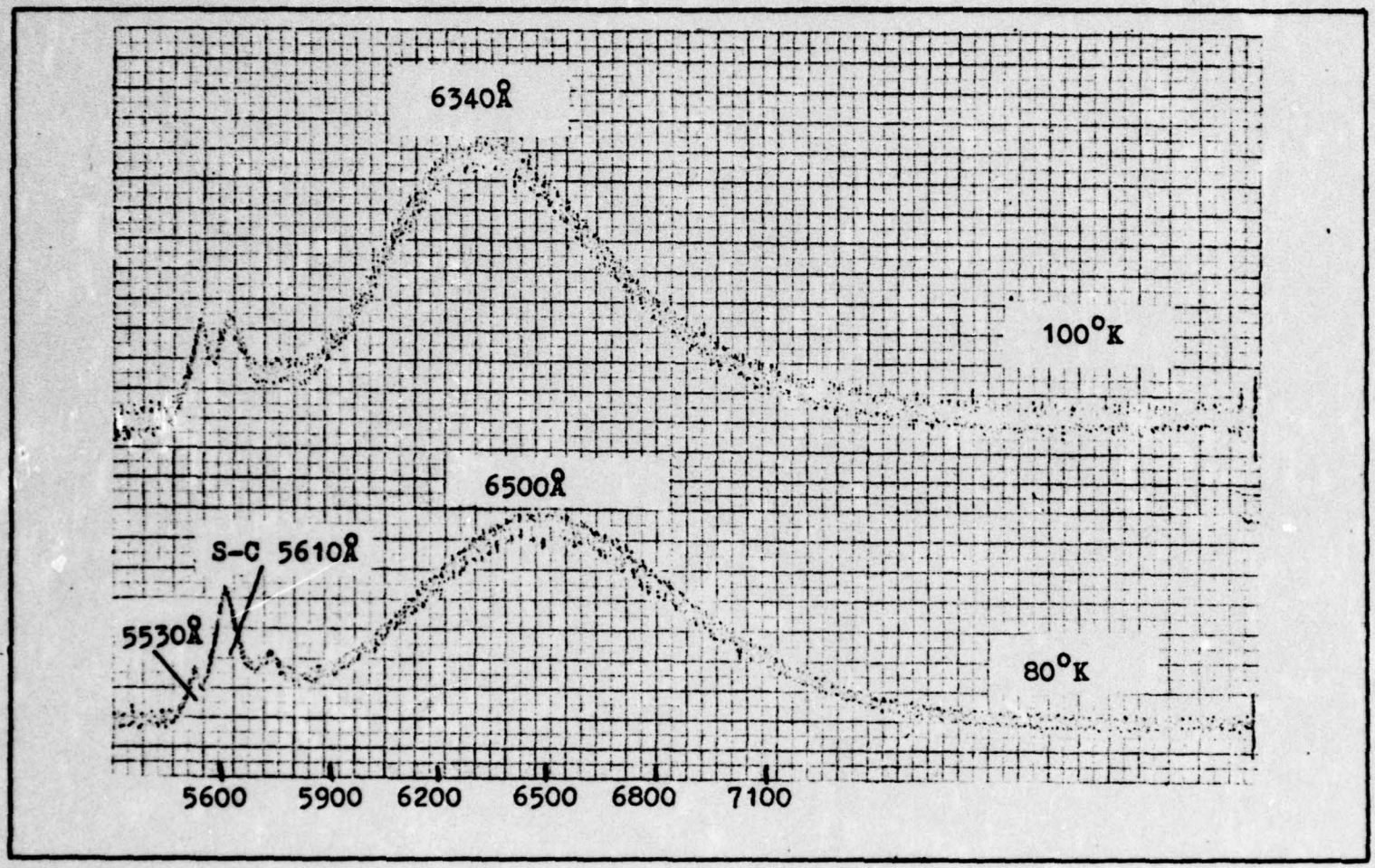

Fig. 10. BSG-12 at 80°, 100°K, 5300Å to 8500Å

Appearing at 80°K is a peak on the high energy slope of the S-C band. Located at 5530Å, this peak has been described as being due to free-bound recombination at either a S or a Si donor (Ref 12, 23). At 100°K (Fig. 10), the free-bound peak increased slightly while the S-C and S-Si/Si-Si bands decreased, and in addition, the S-Si/Si-Si pair band shifted to a higher energy. Since a phonon replica of the free-bound peak was not evident, the free-bound peak was assumed to be due to S donors. Therefore, the S-Si/Si-Si band becomes primarily due to the Si-Si bound-bound recombinations, which explains the shift of the broad band to a higher energy (Ref 9:5640). Also, the S-C pair band shifted to a slightly lower energy; the energy shift is consistent with Eqs (1) and (8). E_G decreases at higher temperatures by Eq (1), and the decreased E_G results in a lower E_{BB} by Eq (8).

In summary, all the spectral features found by a photoluminescence experiment were also evident in the cathodoluminescence study. Several additional peaks were also recorded (A-B, C, and NN peaks) which may indicate a greater sensitivity in the cathodoluminescence procedure. Therefore, results from this report are comparable to those from photoluminescence studies.

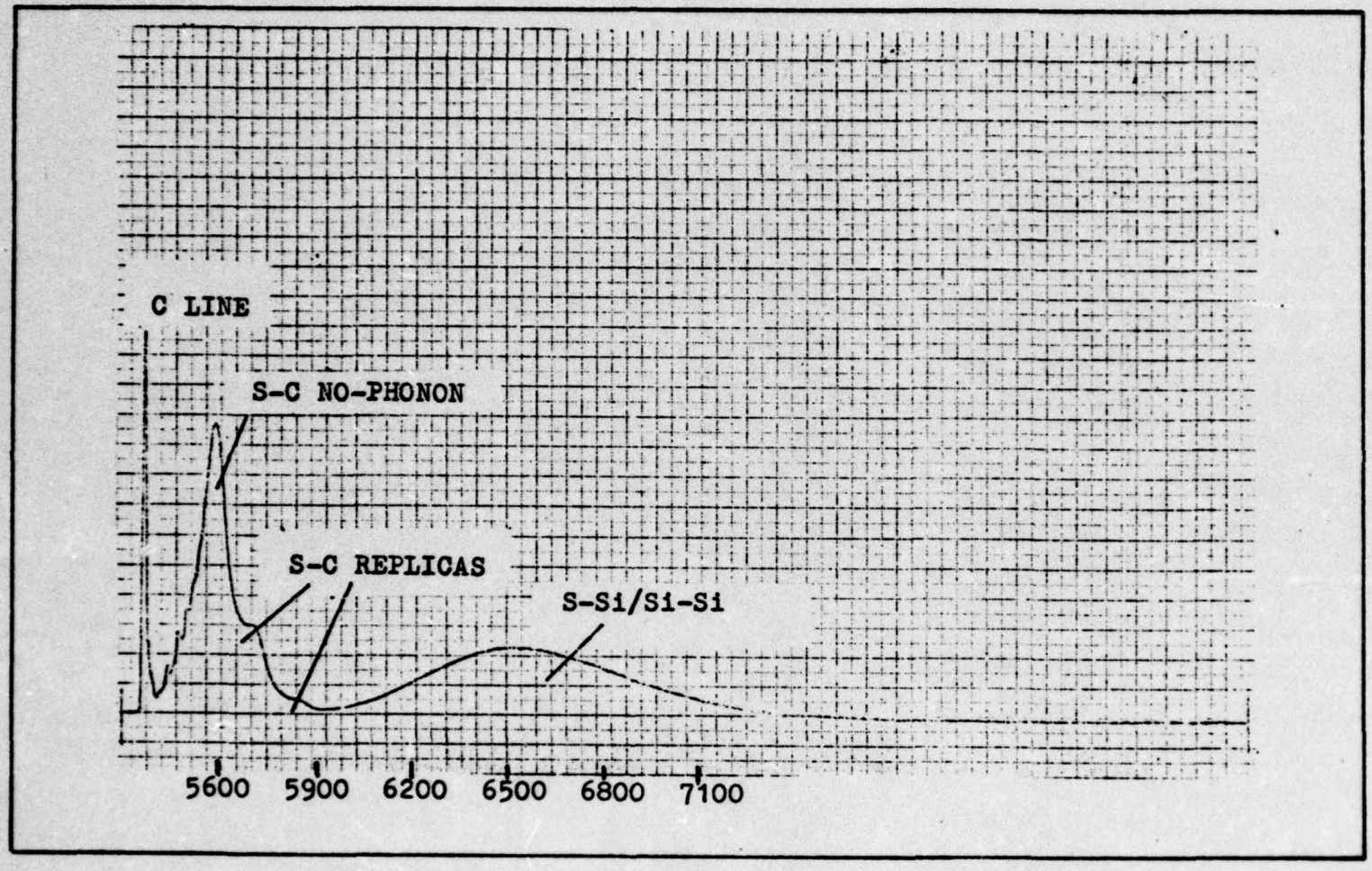

Fig. 11. LPE-67 at 8°K, 5300Å to 8800Å

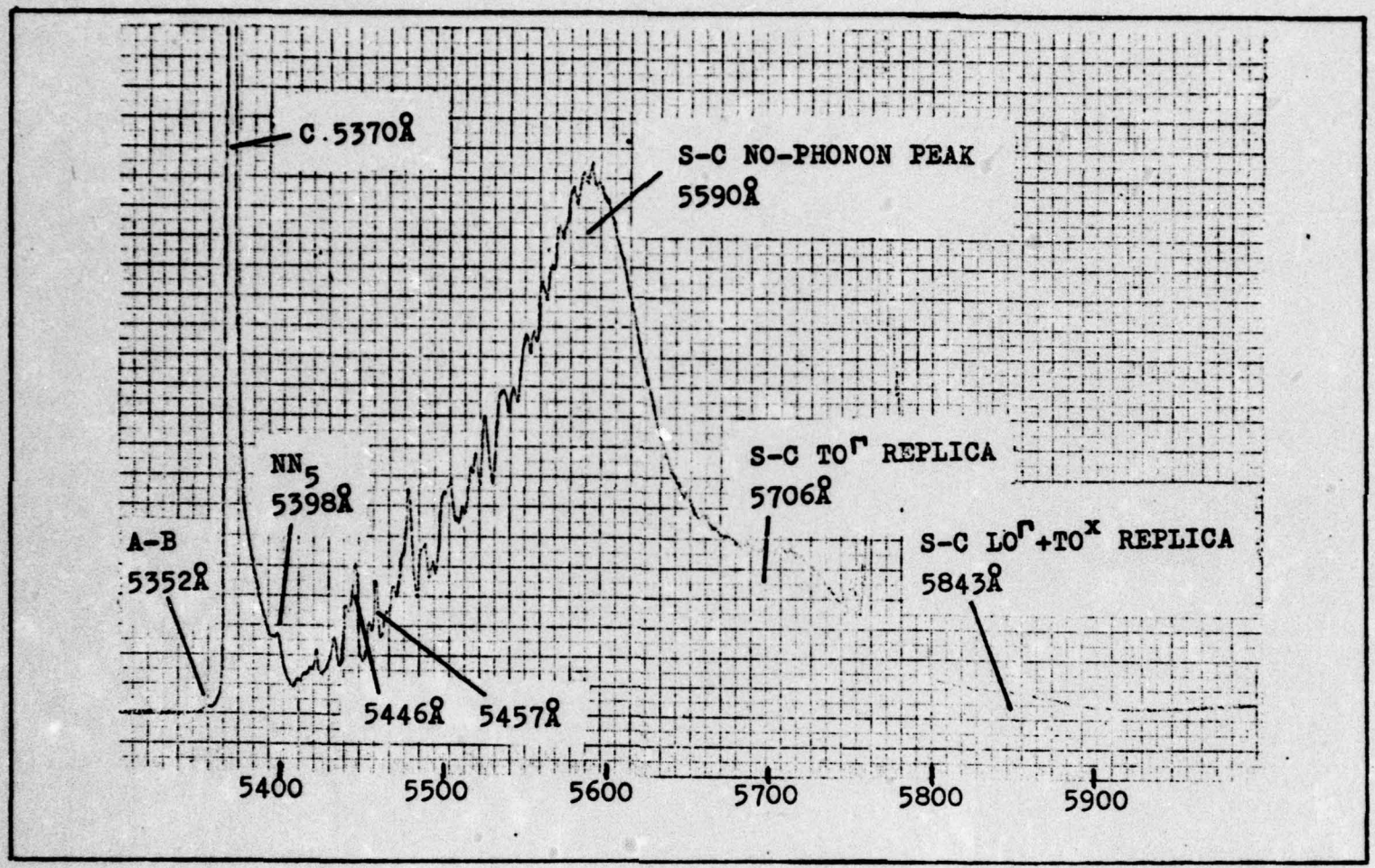

Fig. 12. LPE-67 at 8°K, 5300Å to 6000Å

LPE-67

LPE-67 was an undoped GaP sample grown in a graphite apparatus, and Fig. 11 shows the initial scan at 8°K. A strong C line is the main feature while the S-C pair band with its associated phonon replicas and the S-Si/Si-Si pair band at 6500Å are also prominent.

At higher resolution, Fig. 12 is the 8°K edge emission scan. The C line (5370Å) dominates while the *no-phonon* S-C peak (5590Å) and its associated phonon replicas TO^{Γ} (5706Å) and $LO^{\Gamma} + TO^{X}$ (5843Å) are strong (Ref 7:660). Because LPE-67 exhibited weaker luminescence than BSG-12, the fine structure on the high energy slope of the S-C pair band is not as distinct. However, the type I S-C arrangement can still be determined by the gap between 5446Å and 5457Å. Although one weaker peak exists in this gap, the type II shows several strong peaks in this region; and therefore, the identification is valid (Ref 9:5637). Also present, but weak, is the A-B line (5352Å); the NN_5 peak (5398Å) is evident while NN_4 and NN_3 could again be possibly located in the S-C fine structure.

In LPE-67, the bound exciton lines dominate the spectra while in BSG-12, bound-bound recombinations dominate. In this case, LPE-67 is assumed to be of higher purity than BSG-12. Carbon acceptors, probably due to the graphite growth apparatus, combined with the sulfur donors to form

bound-bound transitions. The broad band at 6500Å is again probably due to S-Si bound-bound recombinations. The band is assumed to be the S-Si pair band because the S-Si band is located at a lower energy than the Si-Si pair band. The presence of the A-B and NN peaks indicates isoelectronic nitrogen impurities; and, because of their relative intensities, a nitrogen concentration approaching 10^{19} cm^{-3} is present (Ref 24:687).

At 15°K (Fig. 13), the C line has diminished in intensity with respect to the S-C pair band, and an overall decrease in intensity is observed. Between 15°K and 60°K, the C line disappeared, but the S-C band continues to dominate the S-Si pair band. The S-Si band shows increasingly better definition, and an accurate wavelength of 6275Å could be established. At 60°K (Fig. 14), the S-Si band dominated the S-C band which shifted toward a slightly lower energy compared to the 15°K scan. High temperature scans (80°, 90°, and 100°K) are displayed in Fig. 15, and the only spectral feature present was the S-Si pair band. As the temperature increased from 80°K to 100°K, the S-Si band shifted toward lower energy (from 6293Å to 6335Å). The shift to lower energy for both the S-C and S-Si pair bands was consistent with Eq (8). As the temperature increased, E_G decreased (Eq (1)) resulting in a lower transition energy E_{BB} and a longer wavelength for both bands.

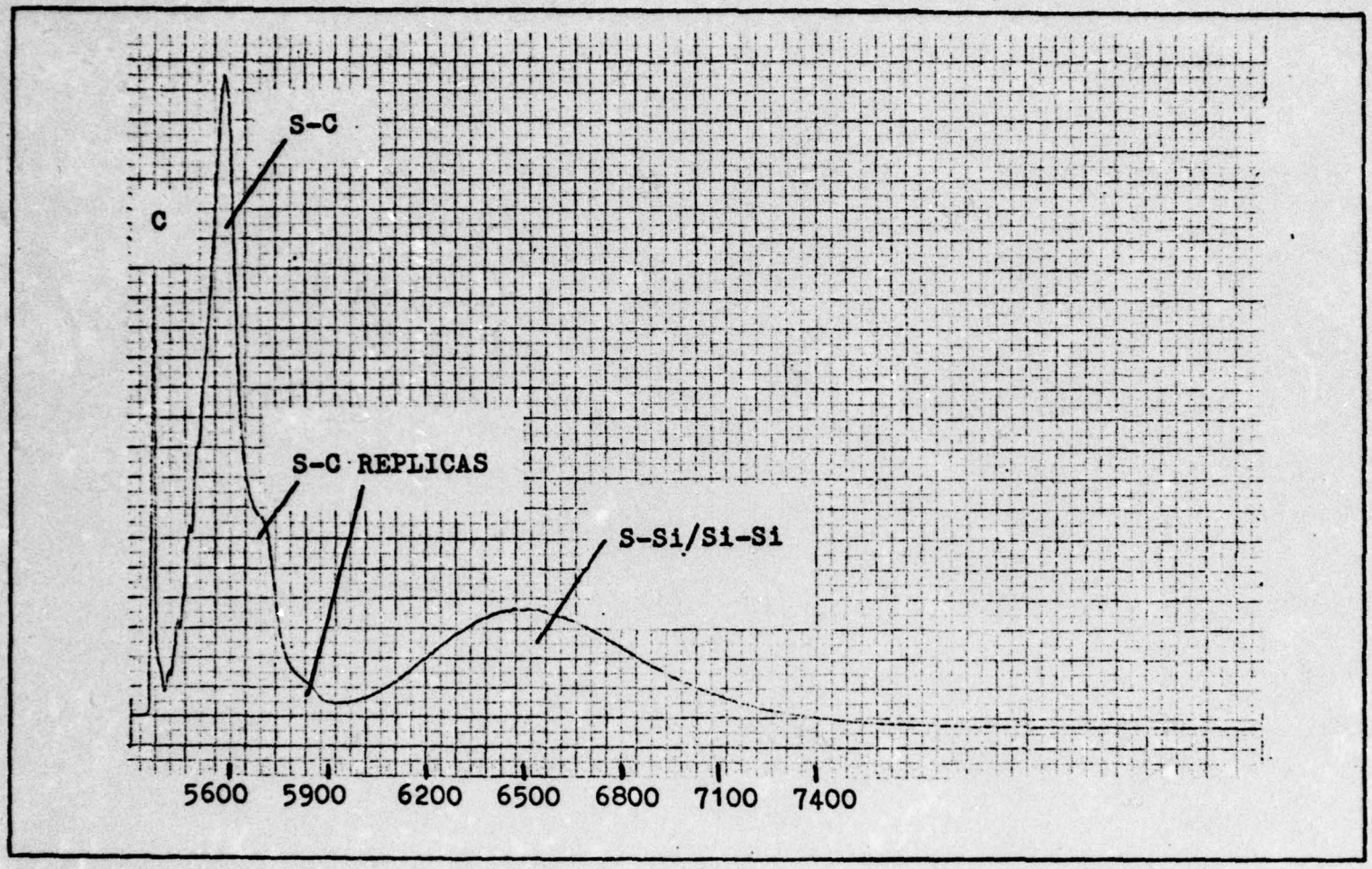

Fig. 13. LPE-67 at 15°K, 5300Å to 8800Å

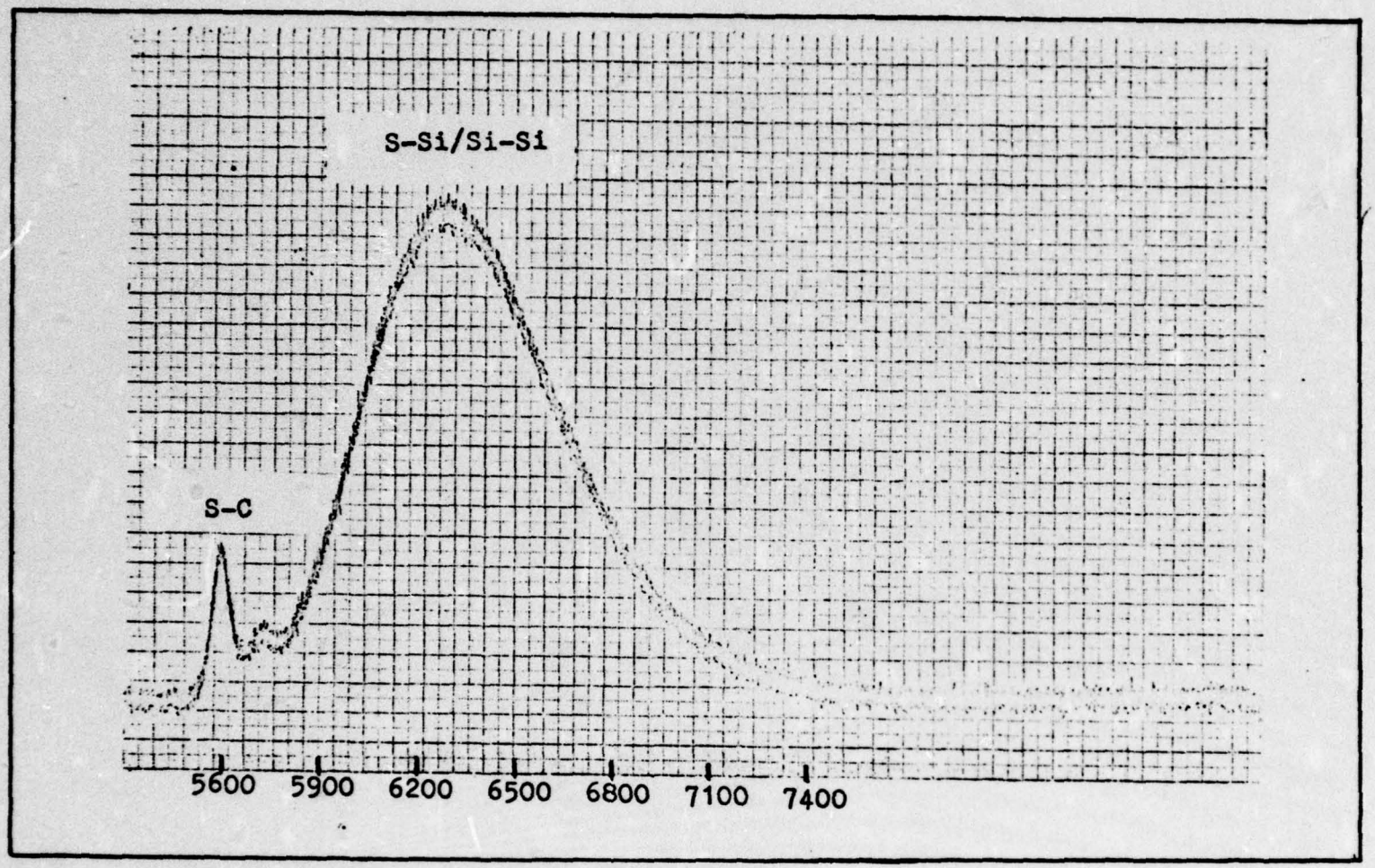

Fig. 14. LPE-67 at 60°K, 5300Å to 8800Å

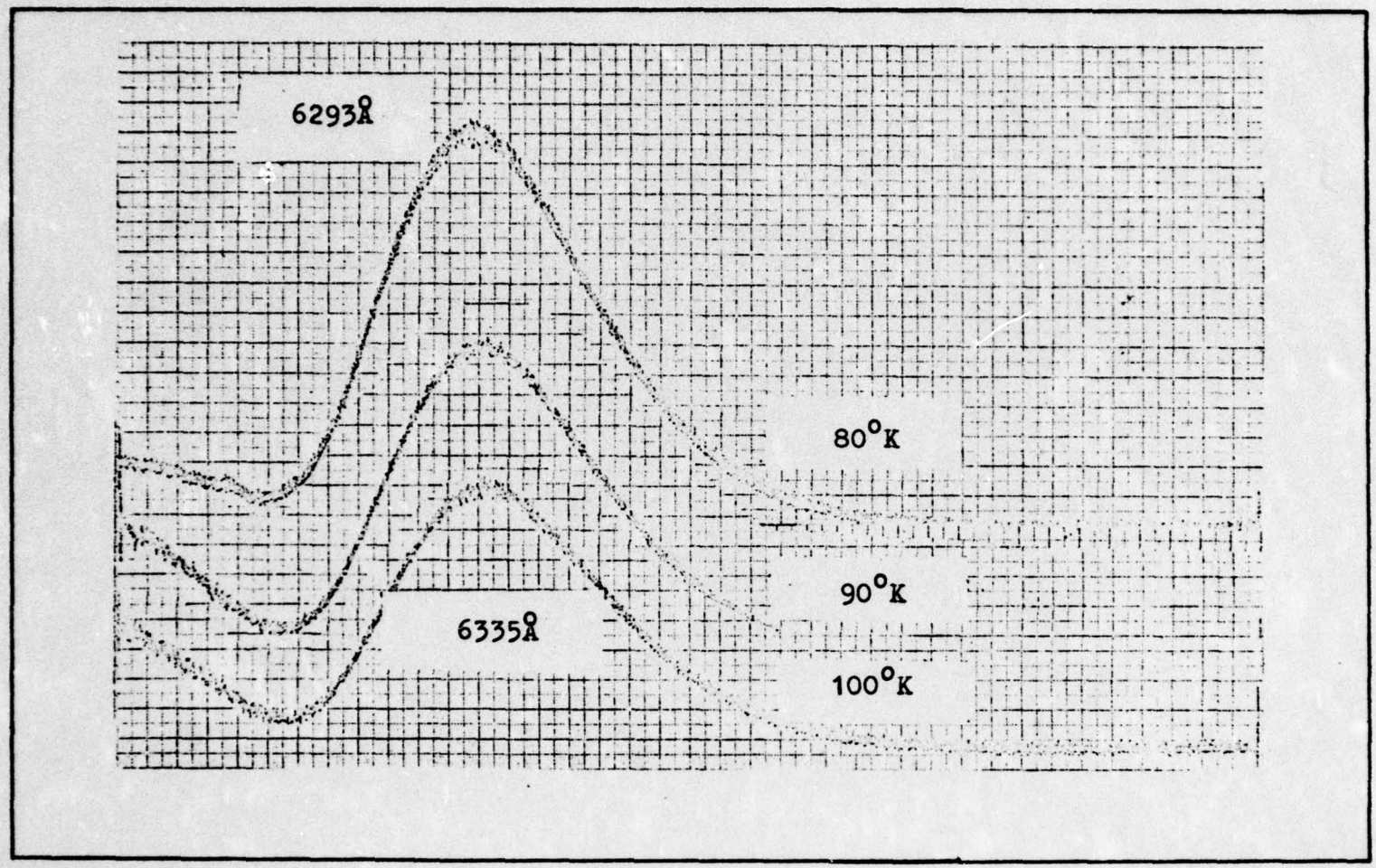

Fig. 15. LPE-67 at 80°, 90°, and 100°K

LPE-68

LPE-68 was a copper doped GaP sample grown in the same apparatus as LPE-67. The luminescence from LPE-68 was less than that from previous samples, and Fig. 16 is the initial 8°K scan. A very strong S-C pair band with phonon replicas dominated the spectra, but an intense broad band is present above 6500Å. The 6500Å broad band is again due to the S-Si bound-bound recombinations. A weak bound exciton peak existed below the S-C no-phonon peak. A small band appeared at 8300Å, but it was due to an experimental discrepancy and was not a legitimate spectral feature.

The edge emission can be observed at higher resolution in Fig. 17; and as with LPE-67, the fine structure on the high energy S-C pair band slope was not very distinct. However, the gap between 5447Å and 5461Å indicated a type I S-C impurity arrangement. Phonon replicas of the S-C no-phonon peak (5591Å) were LO^X (5712Å) and $2LO^\Gamma$ (5859Å). The bound exciton peak (5370Å) was the C line. The NN_5 peak (5398Å) is barely visible, and the peak riding on the high energy slope of the C line was possibly NN_8 (5369Å). The A-B line could not be seen, and other NN peaks may be in the S-C fine structure.

As in BSG-12, the spectra is dominated by the bound-bound recombinations of S-C and S-Si. As in LPE-67, the presence of NN peaks but not the A-B line indicated a nitrogen concentration of about 10^{19} cm^{-3} (Ref 24:687).

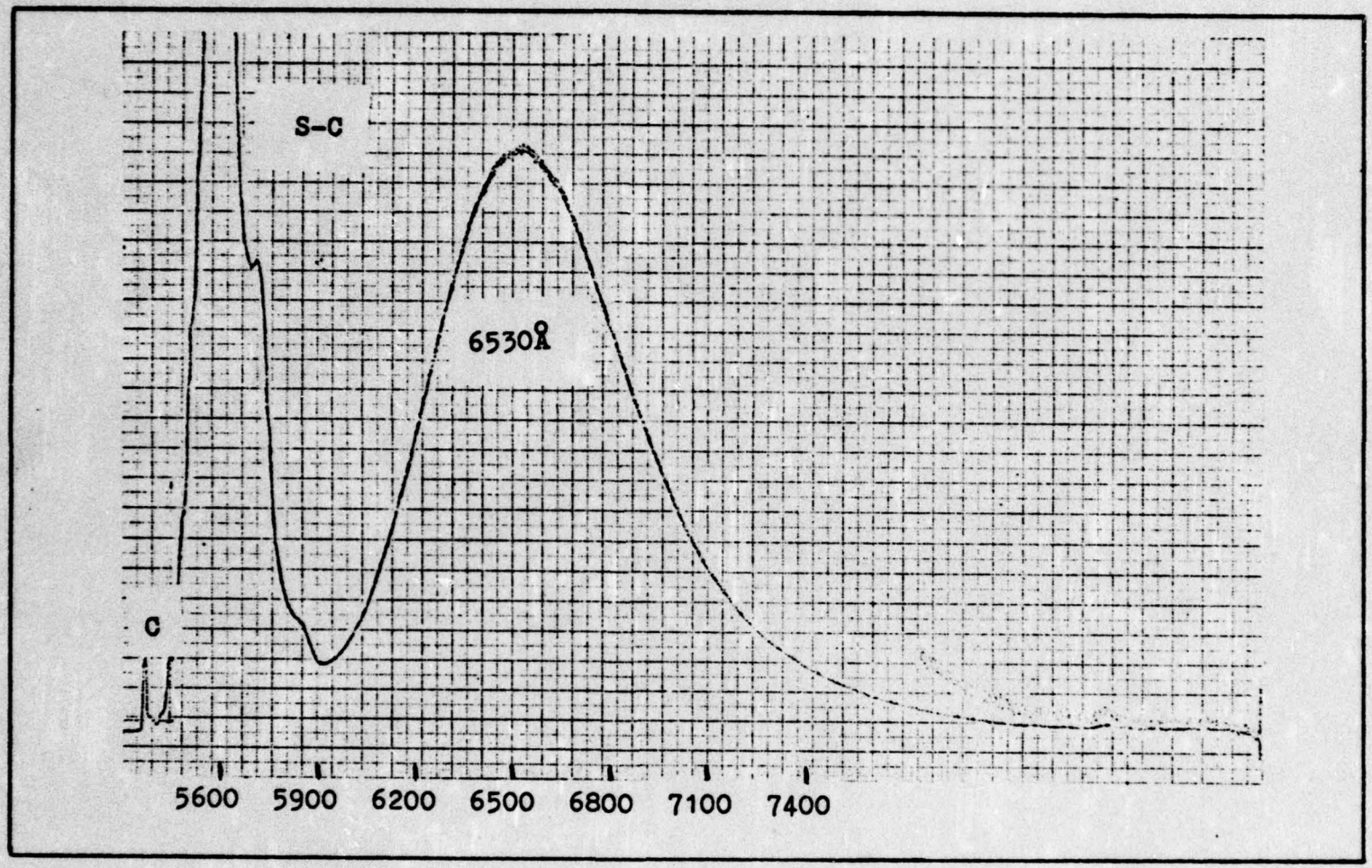

Fig. 16. LPE-68 at 8°K, 5300Å to 8800Å

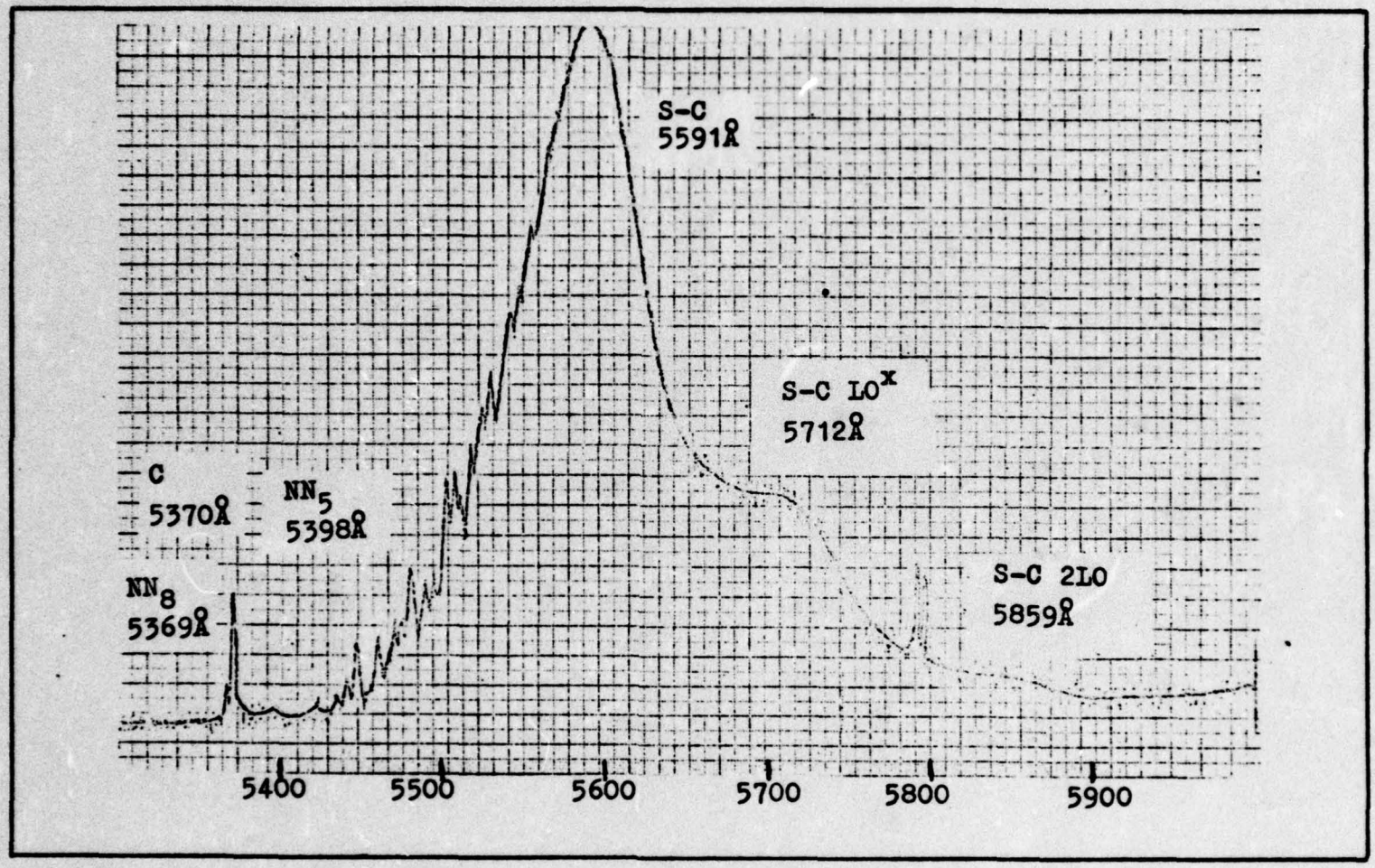

Fig. 17. LPE-68 at 8°K, 5300Å to 6000Å

With increased temperature, the intensity of the spectral features decreased. The C line disappeared; and at 45°K (Fig. 18), the S-C pair band still dominated the broad band (6530Å). However, at 60°K (Fig. 19), the S-C pair band was very small compared to the broad band which has been resolved into two bands (6321Å and 7445Å). The 6321Å band dominated and was due to the S-Si/Si-Si recombinations. The 7445Å broad band was due to the recombinations between the deep acceptor Cu, located on a Ga site, and the shallow donor S, located on a P site (Ref 18:477-478). Further temperature increases to 80°, 90°, and 100°K (Fig. 20) resulted in an overall decrease in intensity. At 80°K, the type II Cu-S pair band dominated the S-Si/Si-Si pair band. Between 80°K and 100°K, both pair bands exhibited the expected behavior for bound-bound spectral features. Both shifted to slightly longer wavelengths which was in agreement with Eq (8).

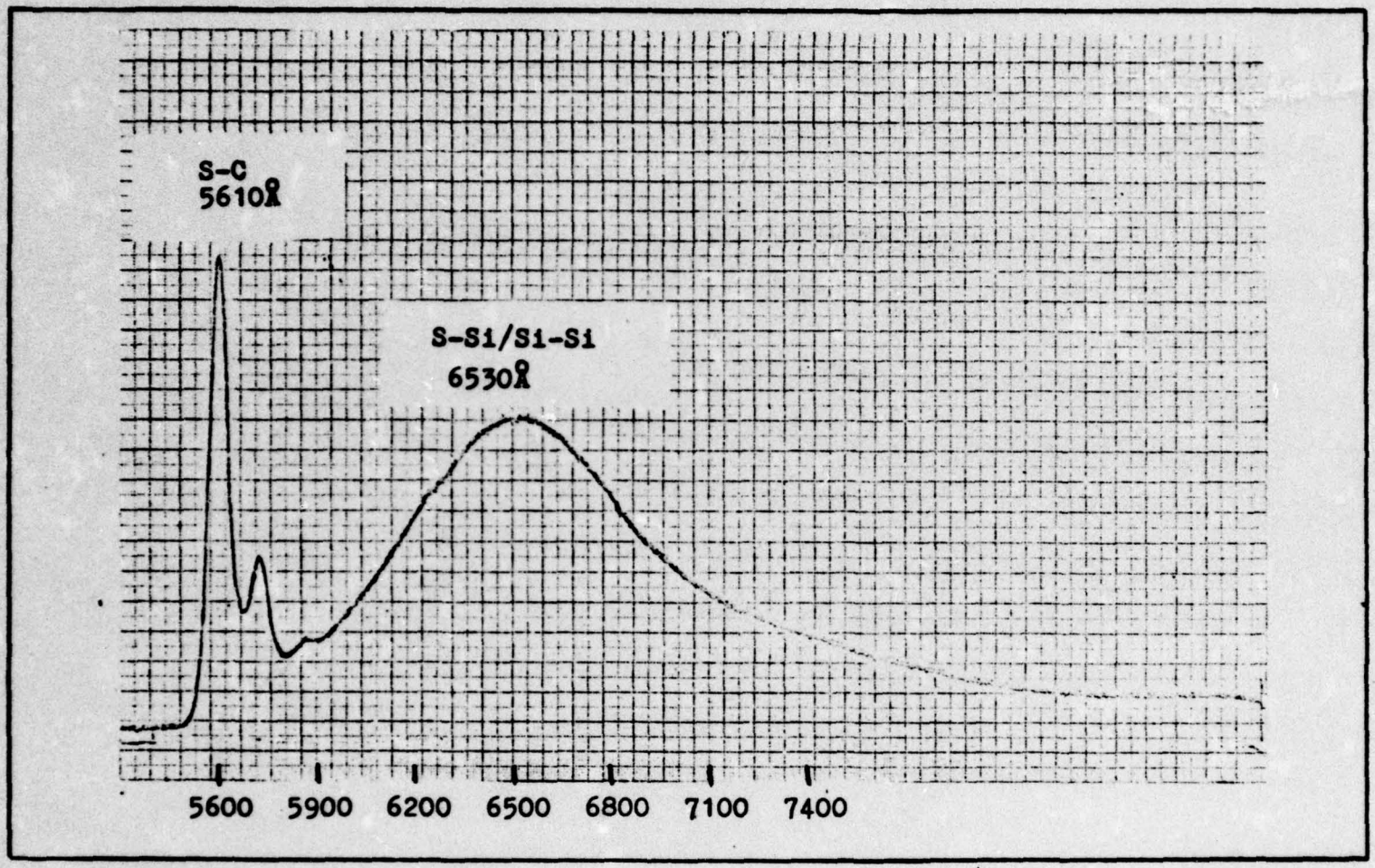

Fig. 18. LPE-68 at 45°K, 5300Å to 8800Å

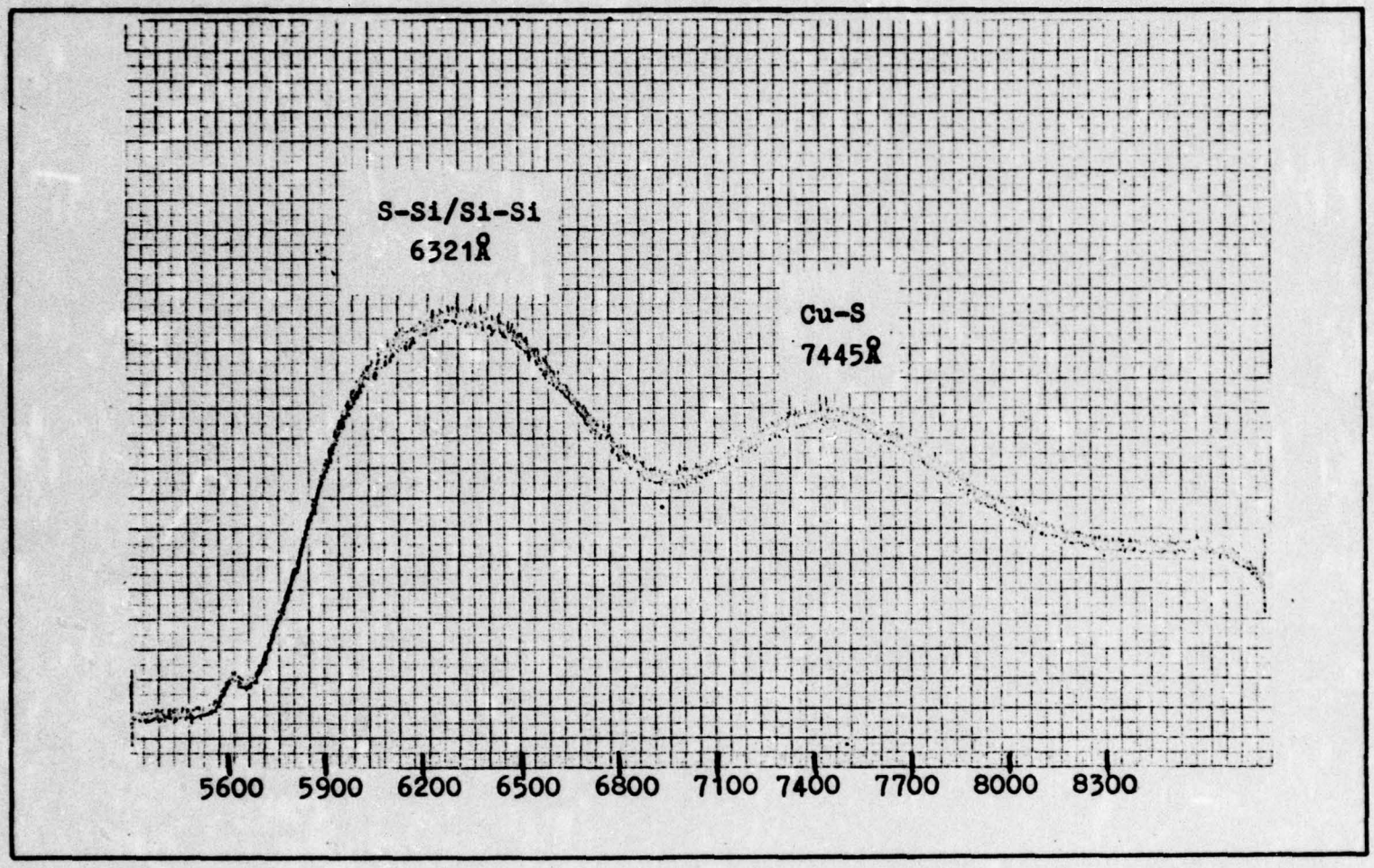

Fig. 19. LPE-68 at 60°K, 5300Å to 8800Å

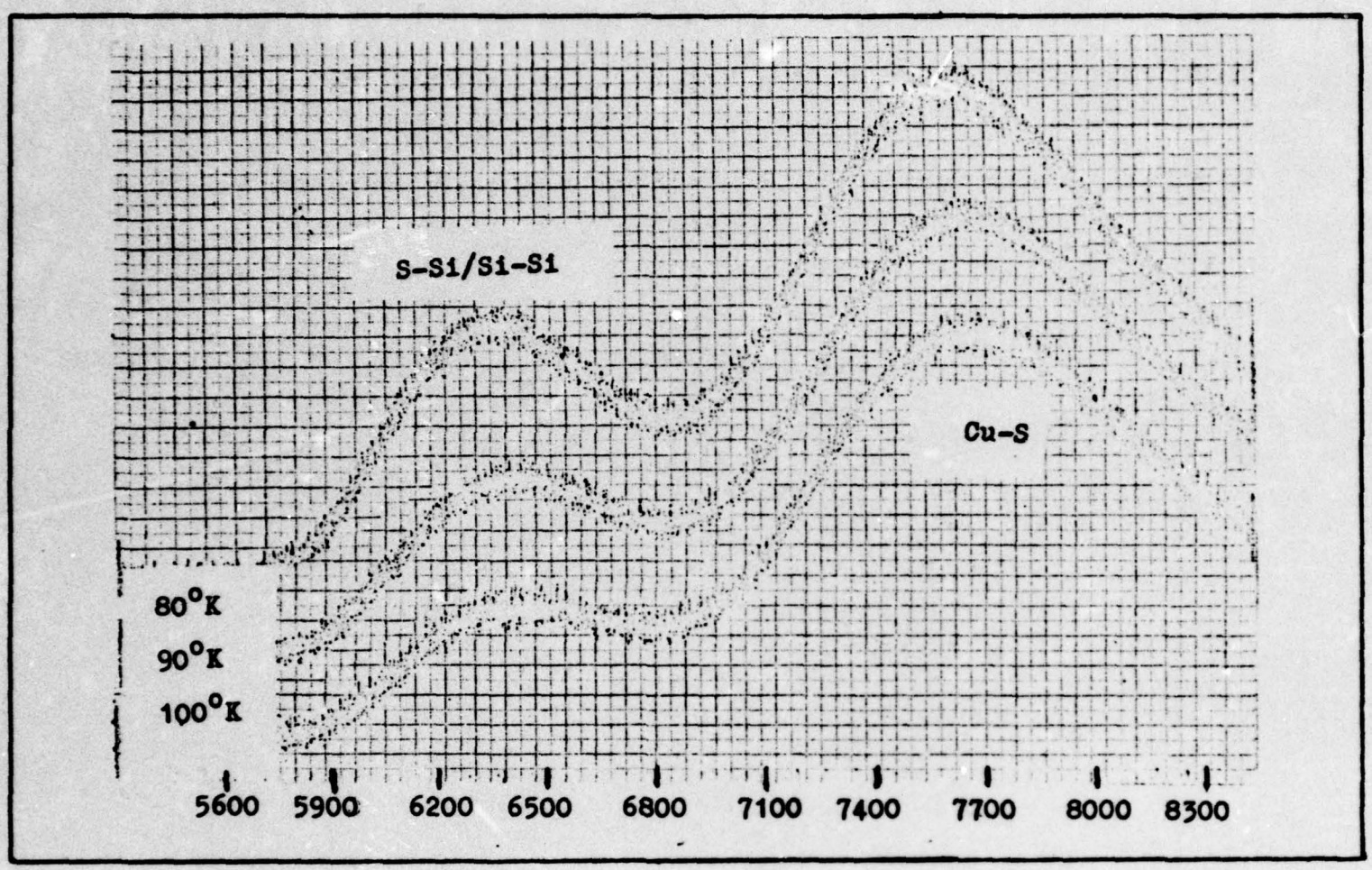

Fig. 20. LPE-68 at 80°, 90°, and 100°K

Sample #1

Sample #1 exhibited strong luminescence only at 8°K and was the weakest sample in terms of luminescence. Fig. 21 is the initial scan at 8°K, and the striking features were the very strong bound exciton peaks. A broad band similar to the one on LPE-68 was present at 6775Å. Although this sample was undoped, this band is located at too long of a wavelength to be due exclusively to the S-Si/Si-Si recombinations. In the region from 5500Å to 5850Å, a band appeared with several smaller peaks on its slopes. This band was a combination of the S-C and Si-C pair bands. The no-phonon Si-C peak (5576Å) and its phonon replicas (5608Å and 5631Å) merge together with the S-C no-phonon peak (5599Å) and its phonon replicas (5714Å and 5834Å) (Ref 9:5644, 24:848).

At higher resolution, the edge emission (Fig. 22) shows little evidence of the Si-C/S-C pair bands. Bound exciton recombinations dominated the spectra, and the C line (5370Å) was the prominent feature. The A-B line (5350Å) and its LO^{Γ} phonon replica (5465Å) were evident as were the NN_3, NN_4, and NN_5 peaks with phonon replicas to NN_4 (5442Å) and NN_3 (5489Å).

Sample #1 appeared to be very high purity because of bound exciton domination of the emission spectra. Appearance of both A-B and the NN peaks indicated a nitrogen concentration of about 10^{18} cm^{-3}. Recombinations involving deep acceptors were indicated by the 6775Å broad band.

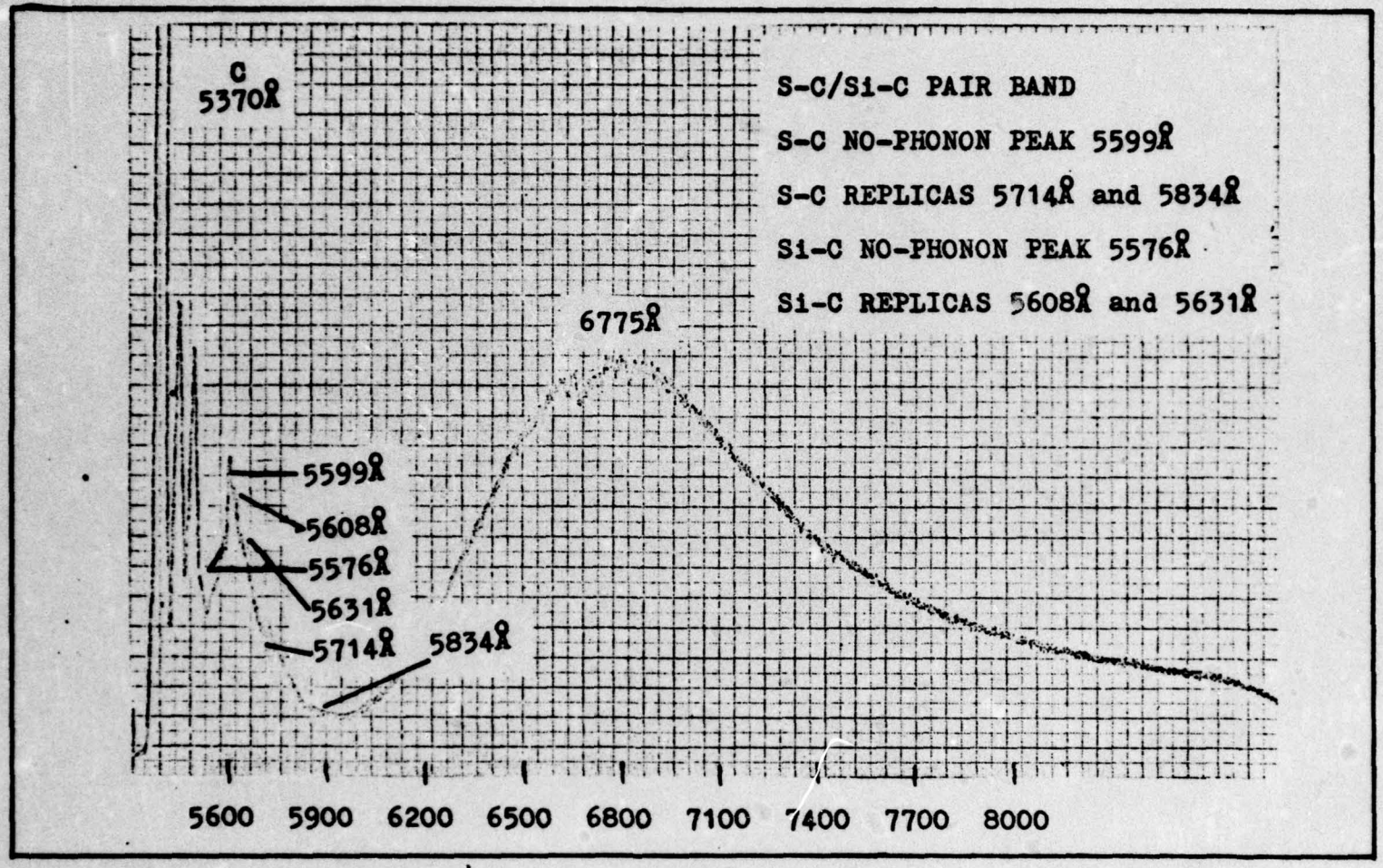

Fig. 21. #1 at 8°K, 5300Å to 8800Å

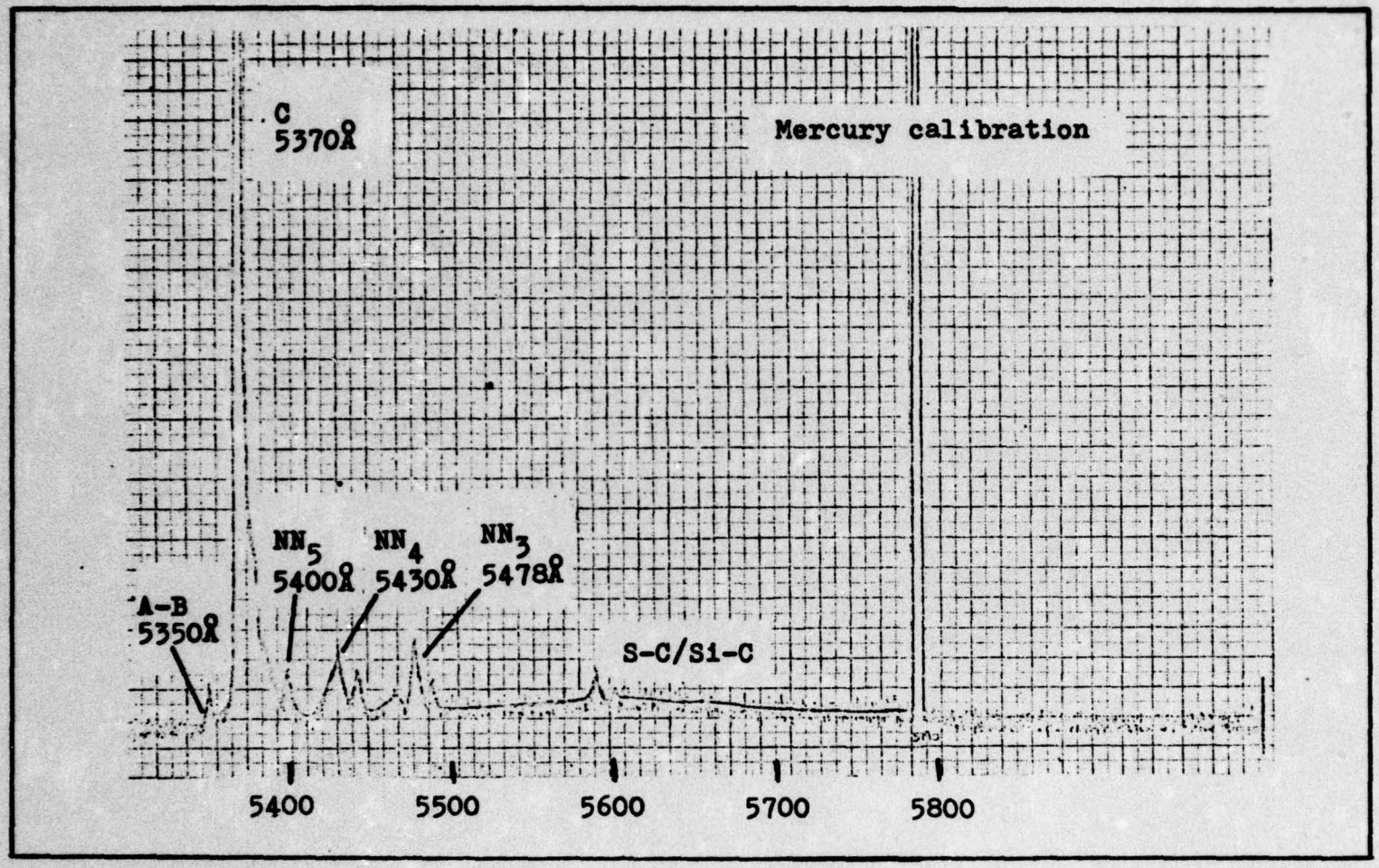

Fig. 22. #1 at 8°K, 5300Å to 6000Å

Sample #1

Sample #1 exhibited strong luminescence only at 8°K and was the weakest sample in terms of luminescence. Fig. 21 is the initial scan at 8°K, and the striking features were the very strong bound exciton peaks. A broad band similar to the one in LPE-68 was present at 6775Å. Although this sample was undoped, this band is located at too long of a wavelength to be due exclusively to the S-Si/Si-Si recombinations. In the region from 5500Å to 5850Å, a band appeared with several smaller peaks on its slopes. This band was a combination of the S-C and Si-C pair bands. The no-phonon Si-C peak (5576Å) and its phonon replicas (5608Å and 5631Å) merge together with the S-C no-phonon peak (5599Å) and its phonon replicas (5714Å and 5834Å) (Ref 9:5644, 24:848).

At higher resolution, the edge emission (Fig. 22) shows little evidence of the Si-C/S-C pair bands. Bound exciton recombinations dominated the spectra, and the C line (5370Å) was the prominent feature. The A-B line (5350Å) and its LO^{Γ} phonon replica (5465Å) were evident as were the NN_3, NN_4, and NN_5 peaks with phonon replicas to NN_4 (5442Å) and NN_3 (5489Å).

Sample #1 appeared to be very high purity because of bound exciton domination of the emission spectra. Appearance of both A-B and the NN peaks indicated a nitrogen concentration of about 10^{18} cm^{-3}. Recombinations involving deep acceptors were indicated by the 6775Å broad band.

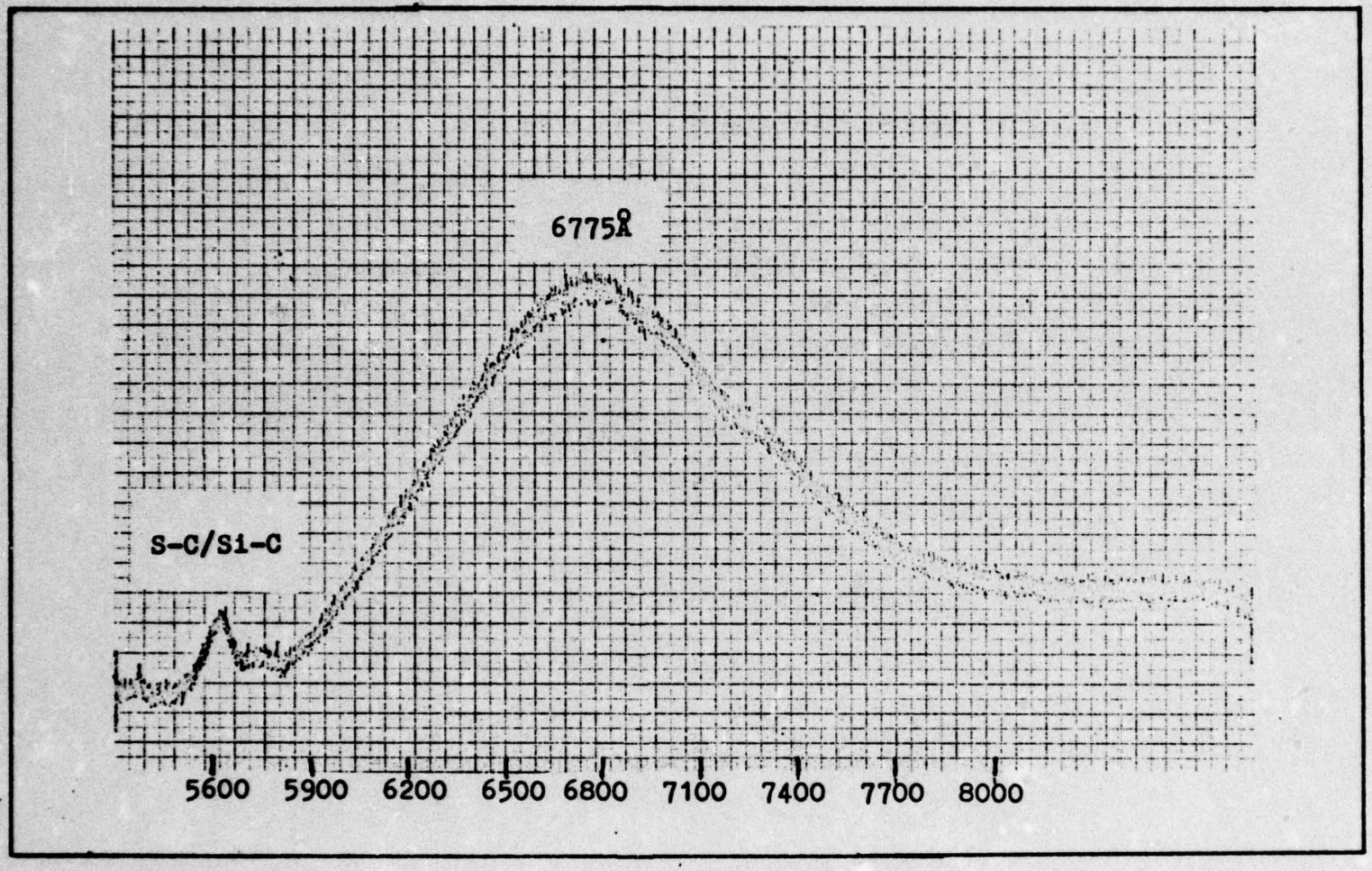

Fig. 23. #1 at 45°K, 5300Å to 8800Å

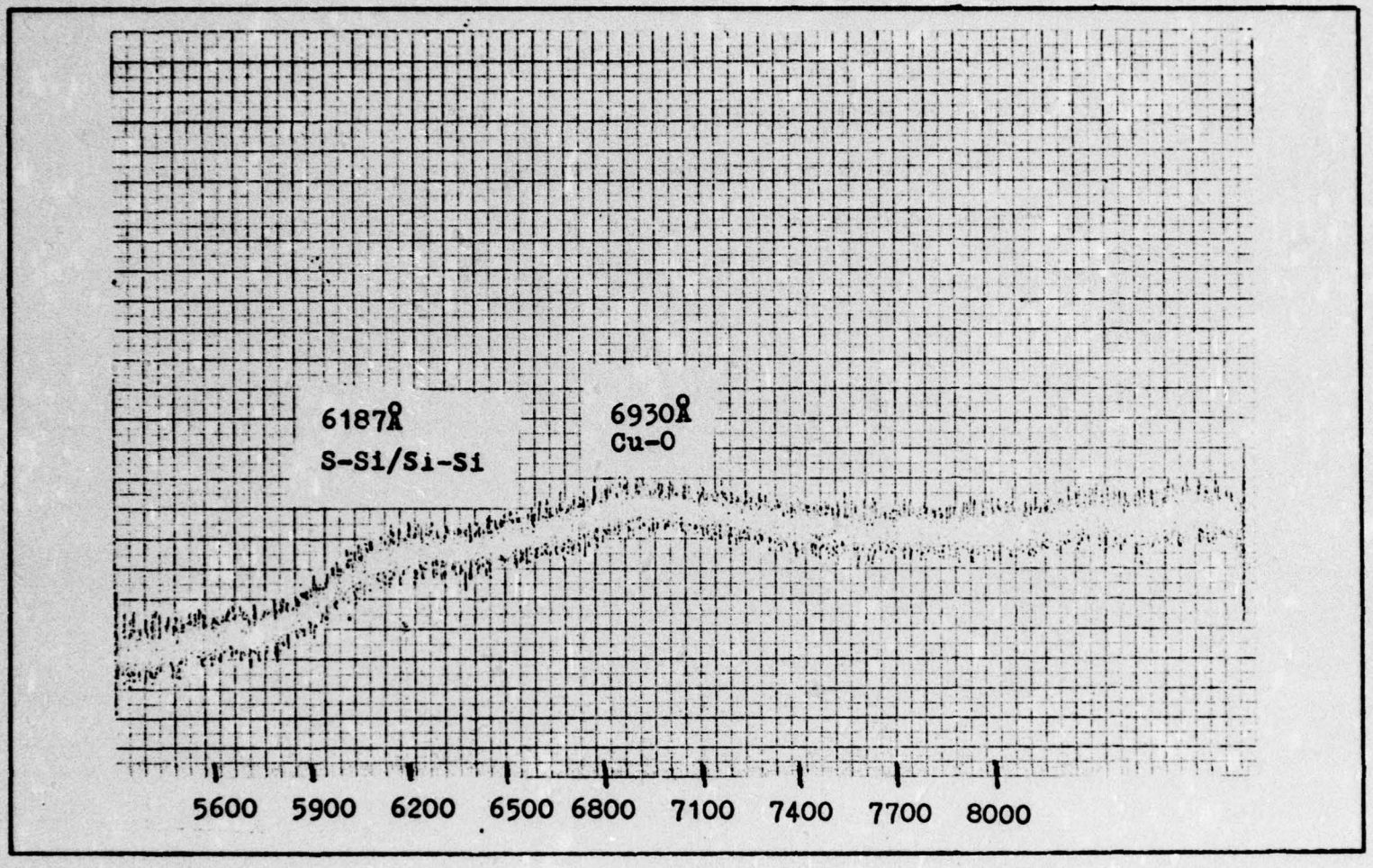

Fig. 24. #1 at 60°K, 5300Å to 8800Å

exciton peak to the strongest pair band at 8°K was used to determine the relative purity of the four samples.

The current gain and Y-scale sensitivity are in the parentheses following each sample, and the magnitude of each spectral feature is in the parentheses following a specific feature.

In only two of the samples did bound exciton recombinations dominate the emission spectra. LPE-67 (0.33×10^8, .25 V/cm) had a C line (12.5 cm) which dominated a S-C pair band (9.5 cm), while #1 (0.33×10^9, .05 V/cm) showed a C line off the graph compared to the 6775Å broad band (13 cm). Apparently #1 is the purer, and comparing the edge emission (Figs. 17 and 22) proves the fact that #1 shows the stronger bound exciton domination. Therefore, based on the purity criterion stated on p. 57-60, #1 is the purest of the four samples and LPE-67 ranks second. Of the other two samples, BSG-12 (0.33×10^7, .1 V/cm) had a S-C pair band (20 cm) that dominated the C line (0.5 cm), while LPE-68 (0.33×10^8, 0.1 V/cm) had a S-C pair band (approximately 35 cm) compared to a C line (2.5 cm). Comparing the ratios of the magnitudes of the pair band to the C line, BSG-12 was 40:1 and LPE-68 was 7:1. Therefore, LPE-68 would rate third in purity and BSG-12 is the least pure.

V. Conclusions and Recommendations

In the course of reviewing the experimental results, several conclusions were drawn. First, analyzing cathodoluminescence proved to be as effective and as sensitive in detecting impurities as the previous photoluminescence studies. It also eliminated one problem of the photoluminescence experiment which is filtering laser lines out of the emission spectra.

In analyzing the four samples, most of the impurities found were common to all four samples. The exceptions were Cu and O in #1, and Cu in LPE-68. The common impurities were S, N, Si, and C. From the literature, all of these would seem to originate in some phase of growth. The growth apparatus for all four samples was made of graphite, and this was the probable source of the carbon. Si and N could also have originated in the starting materials used in growing the samples. At some growth stage in the past, a quartz ampoule or boron nitride boat might have been used, and the residual effects were recorded in this experiment. Sulfur has been identified as a common impurity in the phosphorus used in making GaP.

Sample #1 was identified as the purest of the four samples, based on the criterion described. In fact, all three LPE grown samples were higher purity than BSG-12. Therefore, for high purity GaP, the LPE growth process appears

to be better than the BSG process. However, the GaP starting material and the purity criteria applied are important areas which should be studied.

During the course of this experiment, several other approaches were discussed in order to gain further information. A depth resolved spectroscopy study would show a sample profile for the LPE crystals, while a time resolved study might show which states are responsible for luminescence. In particular, the free-bound transition postulated by Hill and by Pritchard might be positively identified.

Although all impurities were probably identified in this report, several articles in the literature mentioned transitions occurring in the infrared. Using an appropriate detector, the region beyond 8800Å might be explored as part of an experiment.

Two spectral features which appeared in this report are also candidates for further investigation. Sample #1 was undoped, but the emission spectra revealed a band which was identified as the Cu-O pair band. This sample should be studied further to verify or correct this identification. The S-Si/Si-Si pair band should also be studied. The range over which this band has been observed, from 6200Å to 6500Å, might indicate some recombination mechanism is present, but not fully understood.

Bibliography

1. Adler, R.B., et al. Introduction to Semiconductor Physics. New York: John Wiley & Sons, 1964.

2. Auvergne, D., et al. "Phonon-Assisted Transitions in Gallium-Phosphide Modulation Spectra." Physical Review B, 12:1371 (15 August 1975).

3. Aven, M. and J.S. Prener. Physics and Chemistry of II-VI Compounds. Amsterdam: North-Holland Publishing Company, 1967.

4. Boulet, D.L. Depth Resolved Cathodoluminescence of Cadmium Implanted Gallium Arsenide. Unpublished Thesis. Wright-Patterson Air Force Base, Ohio: Air Force Institute of Technology, December 1975.

5. Colbow, K. "Free-to-Bound and Bound-to-Bound Transitions in CdS." Physical Review, 141:742 (January 1966).

6. Daniels, C.R. Pulsed Cathodoluminescence of Ion-Implanted ZnO. Unpublished Thesis. Wright-Patterson Air Force Base, Ohio: Air Force Institute of Technology, March 1975.

7. Dean, P.J. "Absorption and Luminescence of Excitons at Neutral Donors in Gallium Phosphide." Physical Review, 157:655 (May 1967).

8. -----. "Isoelectronic Traps in Semiconductors (Experimental)." Journal of Luminescence, 7:51 (1973).

9. -----. "Optical Properties of the Group IV Elements Carbon and Silicon in Gallium Phosphide." Journal of Applied Physics, 39:5631 (November 1968).

10. -----. "Recombination Processes Associated with 'Deep States' in Gallium Phosphide." Journal of Luminescence, 1,2:398 (1970).

11. Gershenzon, M., et al. "Radiative Transitions Near the Band Edge of Gallium Phosphide." In Proceedings of the International Conference on the Physics of Semiconductors, Exeter, 1962. The Institute of Physics and the Physical Society: London, 1962.

12. Hill, L.A. Luminescence from Copper-Doped and Undoped Gallium Phosphide. Unpublished Thesis. Wright-Patterson Air Force Base, Ohio: Air Force Institute of Technology, December 1975.

13. Hopfield, J.J. "The Quantum Chemistry of Bound Exciton Complexes." In Proceedings of the Seventh International Conference on the Physics of Semiconductors, edited by M. Hulin. Paris: Dunod, 1964.

14. Madelung, O. Physics of III-V Compounds. New York: John Wiley & Sons, 1964.

15. Maeda, K. "Temperature Dependence of Pair Band Luminescence in GaP." Journal of Physics and Chemistry of Solids, 26:595 (1965).

16. McKelvey, J.P. Solid State and Semiconductor Physics. New York: Harper & Row, 1966.

17. Mobsby, C.D., et al. "Intrinsic Recombination from GaP." Journal of Luminescence, 4:29 (1971).

18. Monemar, B. "Bound Exciton Luminescence in GaP:Cu, O." Journal of Luminescence, 5:239 (1972).

19. Morgan, T.N., et al. "Pair Spectra Involving Si Donors in GaP." Physical Review, 180:845 (15 April 1969).

20. Panish, M.B. and H.C. Casey, Jr. "Temperature Dependence of the Energy Gap in GaAs and GaP." Journal of Applied Physics, 40:163 (January 1969).

21. Petersen, P.E., et al. Advanced Development on Gallium Phosphide Materials for Satellite Attitude Sensors. Honeywell Inc. Corporate Research Center Interim Report. 15 May 1975 - 28 November 1975. Wright-Patterson Air Force Base, Ohio: Air Force Materials Laboratory, January 1976.

22. Pierce, B.J. Luminescence and Hall Effect of Ion Implanted Layers in ZnO. Unpublished Dissertation. Wright-Patterson Air Force Base, Ohio: Air Force Institute of Technology, September 1974.

23. Pritchard, H.H., Photoluminescence of Gallium Phosphide. Unpublished Thesis. Wright-Patterson Air Force Base, Ohio: Air Force Institute of Technology, June 1976.

24. Thomas, D.G., et al. "Isoelectronic Traps Due to Nitrogen in Gallium Phosphide." Physical Review Letters, 15:857 (29 November 1965).

25. Thomas, D.G. and J.J. Hopfield. "Isoelectronic Traps Due to Nitrogen in Gallium Phosphide." Physical Review, 150:680 (October 1966).

26. Thomas, D.G., et al. "Pair Spectra and 'Edge' Emission in Gallium Phosphide." Physical Review, 133:A269 (6 January 1964).

27. Willardson, R.K. and A. Beer, editors. Semiconductors and Semimetals. Vol. II: Physics of III-V Compounds. New York: Academic Press, 1966.

Vita

James C. Slavicek was born on August 15, 1947 in Oak Park, Illinois, the son of James and Josephine Slavicek. He attended Riverside-Brookfield High School in Riverside, Illinois and graduated in 1965. Capt. Slavicek then attended the University of Illinois-Chicago and received a Bachelor of Science degree in Physics in 1969. Entering the Air Force in January, 1970, he was commissioned in April of that year and assigned to Mather AFB, California. After completing both navigator and electronic warfare training, he was assigned to the 449th Bomb Wing (SAC) at Kincheloe AFB, Michigan. In June, 1975, Capt. Slavicek was assigned to the Air Force Institute of Technology.

Permenent address: 3136 Raymond Ave.
Brookfield, Illinois 60513

UNCLASSIFIED

SECURITY CLASSIFICATION OF THIS PAGE (When Data Entered)

REPORT DOCUMENTATION PAGE		READ INSTRUCTIONS BEFORE COMPLETING FORM
1. REPORT NUMBER GEP/PH/76-9	2. GOVT ACCESSION NO.	3. RECIPIENT'S CATALOG NUMBER
4. TITLE (and Subtitle) DETERMINING IMPURITIES IN GALLIUM PHOSPHIDE BY ANALYZING CATHODOLUMINESCENCE		5. TYPE OF REPORT & PERIOD COVERED MS Thesis 6. PERFORMING ORG. REPORT NUMBER
7. AUTHOR(s) James C. Slavicek Capt		8. CONTRACT OR GRANT NUMBER(s)
9. PERFORMING ORGANIZATION NAME AND ADDRESS Air Force Institute of Technology (AFIT-EN) Wright-Patterson AFB, Ohio 45433		10. PROGRAM ELEMENT, PROJECT, TASK AREA & WORK UNIT NUMBERS Project 73710233
11. CONTROLLING OFFICE NAME AND ADDRESS AFML/LPO Air Force Materials Laboratory Wright-Patterson AFB, Ohio 45433		12. REPORT DATE December, 1976 13. NUMBER OF PAGES 66
14. MONITORING AGENCY NAME & ADDRESS(if different from Controlling Office)		15. SECURITY CLASS. (of this report) Unclassified 15a. DECLASSIFICATION/DOWNGRADING SCHEDULE

16. DISTRIBUTION STATEMENT (of this Report)

Approved for public release; distribution unlimited

17. DISTRIBUTION STATEMENT (of the abstract entered in Block 20, if different from Report)

18. SUPPLEMENTARY NOTES

Approved for public release; IAW AFR 190-17

JERRAL F. GUESS, CAPT, USAF
Director of Information

19. KEY WORDS (Continue on reverse side if necessary and identify by block number)

Gallium Phosphide
Cathodoluminescence

20. ABSTRACT (Continue on reverse side if necessary and identify by block number)

The cathodoluminescence emission spectra of four GaP samples, three grown by a liquid phase epitaxial(LPE) process and the fourth bulk solution grown(BSG), was studied in order to identify impurities present in the samples. The samples were excited by a 20 kV, 1.0 microampere electron beam; and the spectra, photoelectrically detected, were recorded at various sample temperatures between 8°K and 100°K using liquid helium and liquid nitrogen as coolants. The impurities, identified

DD FORM 1 JAN 73 1473 EDITION OF 1 NOV 65 IS OBSOLETE

UNCLASSIFIED

SECURITY CLASSIFICATION OF THIS PAGE (When Data Entered)

20. by comparison with the literature, were S, N, C, Si, and O. In addition, two of the samples showed the presence of Cu although only one sample was intentionally Cu doped. The cathodoluminescence procedure was found to be as sensitive and effective as the photoluminescence procedure in detecting impurities, and the LPE process appeared to produce the purest samples.